ORCA – Online Research @ Cardiff

This is an Open Access document downloaded from ORCA, Cardiff University's institutional repository:https://orca.cardiff.ac.uk/id/eprint/101009/

This is the author's version of a work that was submitted to / accepted for publication.

Citation for final published version:

Mu, Qing, Liang, Jun , Zhou, Xiaoxin, Li, Chuanyue and Li, Yalou 2017. Systematic evaluation for multi-rate simulation of DC Grids. International Journal of Electrical Power and Energy Systems 93 , pp. 119-134. 10.1016/j.ijepes.2017.05.020

Publishers page: https://doi.org/10.1016/j.ijepes.2017.05.020

Please note:
Changes made as a result of publishing processes such as copy-editing, formatting and page numbers may not be reflected in this version. For the definitive version of this publication, please refer to the published source. You are advised to consult the publisher's version if you wish to cite this paper.

This version is being made available in accordance with publisher policies. See http://orca.cf.ac.uk/policies.html for usage policies. Copyright and moral rights for publications made available in ORCA are retained by the copyright holders.

Manuscript Details

Manuscript number	IJEPES_2016_1809
Title	Systematic Evaluation for Multi-rate Simulation of DC Grids
Article type	Research paper

Abstract

With wide applications of power electronic devices in modern power systems, simulation using traditional electromechanical and electromagnetic tools suffers low speed and imprecision. Multi-rate methods can enhance efficiency of simulation by decreasing the scale of systems in small time-steps. However, the existing traditional methods for multi-rate simulation suffer the problems of instability and simulation errors. These have hindered the application of multi-rate simulation in power industry. Therefore theoretical evaluation on different multi-rate simulation methods is crucial to understand the feasibility and limitation of the methods, and to contribute to overcome the drawbacks of the traditional methods. In this paper, the multi-rate simulation performance based on two traditional technologies and a Modified Thevenin Interface are evaluated to provide an overall feasibility of multi-rate algorithms in the power simulation. The Modified Thevenin Interface is proposed to overcome the drawbacks in synchronization. Three theorems are proposed and proved for theoretically analyzing the stability of the simulation methods. Error analyses of the multi-rate methods are performed to identify the relationships between errors and simulation conditions. Besides, the accuracy and efficiency performance in a practical project of VSC-MTDC shows the feasibility and necessity by using multi-rate simulation. Through the theoretical analysis, the issues of stability and accuracy of multi-rate simulation for the DC grids have been better understood, based on which an improved simulation algorithm has been proposed to overcome these issues. Long-term system dynamics of large-scale systems containing DC grids and fast transients of HVDC converters can be investigated simultaneously with high speed and sufficient accuracy.

Keywords	Electromagnetic transient analysis, Power System Simulation, Parallel Algorithm, Multi-rate Interface, Different Rates, Multi-terminal VSC-HVDC
Corresponding Author	Qing Mu
Corresponding Author's Institution	Cardiff University
Order of Authors	Qing Mu, Jun Liang, Xiaoxin Zhou, Chuanyue Li, Yalou Li

Submission Files Included in this PDF

File Name [File Type]

cover_letter V2.doc [Cover Letter]

Review_IndV10.docx [Response to Reviewers]

multirate simulation for DC grid0508.docx [Manuscript File]

Highlights.doc [Highlights]

To view all the submission files, including those not included in the PDF, click on the manuscript title on your EVISE Homepage, then click 'Download zip file'.

Journal of Advanced Research

Cover Letter

Manuscript title:

Systematic Evaluation for Multi-Rate Simulation of DC Grids

***Short running title*:**

Evaluation for Multi-Rate Simulation

What does the current manuscript add to the existing knowledge? (Research Highlights)

1- Three theorems for the stability of three typical multi-rate simulation algorithms have been proposed and proved.
2- The error of three typical multi-rate simulation algorithms has been modelled.
3- The backward synchronization for the Thevenin equivalent interface has been proposed to overcome the challenge of synchronization.
4- Three typical multi-rate simulation algorithms have been compared to illustrate that the modified Thevenin equivalent interface is the most stable and accurate.
5- The multi-rate simulation algorithm has been used in the studies of DC grids, which achieve the great improvement of the simulation speed.

We affirm that the submission represents original work that has not been published previously and is not currently being considered or submitted to another journal, until a decision has been made. Also, we confirm that each author has seen and approved the contents of the submitted manuscript.

Signature (on behalf of all co-authors (if any))

Corresponding author

Name: Qing Mu

Affiliation: Cardiff University

Tel.:+8618612425770

Fax:

E-mail address: muqing_zju@163.com

Submission date: 24th, Aug

Responses：

The authors would like to thank the reviewers for their constructive comments. The responses to each comment have been carefully prepared by the authors and are given as below. Corresponding modifications of the paper have also been indicated.

Reviewer 1:

> The abstract can be revised to include more details of the proposed approach. Authors can improve the abstract by including the existing challenges, motivations and outcomes of the paper. Furthermore, it is suggested that authors add 1-2 sentences to motivate this study before stating the novelty of their work.

The abstract has been revised according to the suggestions.

The existing challenges and motivations are included in Abstract.

"However, the existing traditional methods for multi-rate simulation suffer the problems of instability and simulation errors. These have hindered the application of multi-rate simulation in power industry. Therefore theoretical evaluation on different multi-rate simulation methods is crucial to understand the feasibility and limitation of the methods, and to contribute to overcome the drawbacks of the traditional methods."

The outcomes are included in Abstract.

"Through the theoretical analysis, the issues of stability and accuracy of multi-rate simulation for the DC grids have been better understood, based on which an improved simulation algorithm has been proposed to overcome these issues. Long-term system dynamics of large-scale systems containing DC grids and fast transients of HVDC converters can be investigated simultaneously with high speed and sufficient accuracy.

> Introduction section is incomplete. It should include four key components: 1.1.motivation, 1.2. literature survey, 1.3. contributions, and 1.4 the structure of paper. Please modify this section accordingly.

The structure of the Introduction has been revised according to your constructive suggestions. Please refer to the paper for the detailed content.

> Authors are encouraged to add nomenclature in the first section to include are parameters, variables, and abbreviations.

The nomenclature has been added in Page 2 and Page3 according to your constructive suggestions. Please refer to the paper for the detailed content.

> Please add a list of key contributions of this study in the newly-added subsection 1.3. It is not clear for the readers whether the authors proposed some theorems or they just applied some available methods to a system?

The key contributions have been listed in 1.3 Contribution of the Introduction, in Line 9, Page 5, according to your supportive suggests.

"This paper is to provide the systematic evaluation of the multi-rate simulation methods and investigate the stability and accuracy. The major contributions are listed as below:

1. An improved multi-rate method based on the Thevenin equivalent circuit, named Modified Thevenin Equivalent Interface (MTI), is proposed to overcome the issues of synchronization the in multi-rate simulation.

2. Three theorems have been proposed and proved to illustrate the stability characteristics of ITI, TLI and MTI.

3. The simulation errors using ITI, TLI and MTI have been analytically evaluated and the factors of these errors have been obtained.

4. The systematical analysis and comparisons of ITI, TLI and MTI have been performed.in terms of stability and accuracy.

Authors are encouraged to illustrate the results of table I using some plots to make it easy to understand.

The Table I has been replaced by a clear figure, as Fig.18 in Page 19, according to your constructive suggestions.

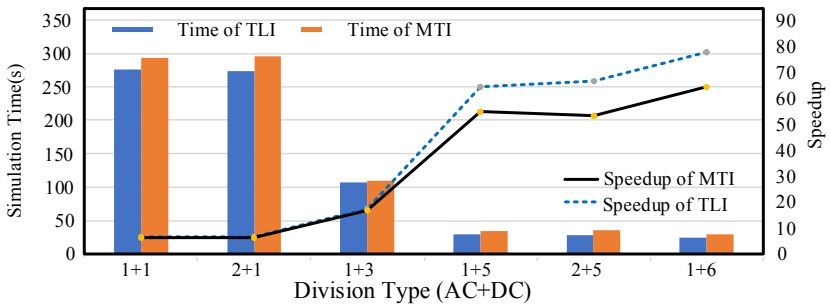

Fig. 1 Computation Time Comparison of different subsystem divivision types.

Furthermore, the figure has been explained in Line 10 from bottom, Page 18.

"The detailed comparison of different dividing schemes is illustrated in Fig. 18. The label in the axis of X represents the division type, (number of AC subsystems + number of DC subsystems). The PSCAD software runs about 1860s for 1s period of simulation as the computation time base."

According to theorem 2" If the simulation of TLI with a single rate is stable, and the divided fast and slow subsystems are also absolutely stable, then the multi-rate simulation algorithm without interpolation is stable as long as all the multiple rates are not larger than the single rate.". Please provide thorough explanations about the assumptions of this theorem.

The clear explanation of the assumptions is added in Line 6 from bottom, Page 11.

"The assumption of this theorem includes that:

- A system is divided into subsystems;
- Stable simulation can be achieved for the subsystems connected through TLI interface using the same time-steps for all subsystems, called a single rate, H. This means that the state transfer matrix in an equation, similar to (21), has the norms less than 1.
- Each subsystem is asymptotically stable, which means that the A11 and A22 in (30) have norms less than 1.
- Different simulation time-steps, which are not larger than the single rate H, are used for

subsystems. Fast subsystems have small time-steps and slow subsystems have relatively large time-steps

When the above assumptions are met, stable simulation can be achieved for the fast and slow subsystems connected through TLI."

In addition, the word "absolutely" in Theorems 1, 2 and 3 is not accurate enough, the "asymptotically" is more accurate. Therefore, the "absolutely" has been replaced with "asymptotically" in the three theorems.

Quality of figures 8, 10, 11, 12, 13, 14, and 15 requires improvement. The font size should be justified with the text and clear to read.

Figures 6,7,8,10,11,12,13,14,15,16,19 and 20 are redrawn in the paper to improve the figure quality.

In order to make the conclusion section more clear, authors need to include the point-by-point findings of this article. The current conclusion is written very wide and it is not easy to maintain the key findings.

The conclusion has been revised and the key findings have been listed.

" The key findings of the study include

1. An improved method, Modified Thevenin Interface (MTI) is proposed to overcome the drawbacks in synchronization of the original Thevenin Interface.

2. Three theorems about ITI, TLI and MTI are proposed and proved in theoretically. From these theorems, it has been found that the stability of multi-rate simulation using these interfaces is only associated with the stability of single rate parallel simulation using these interfaces. The stability of MTI is only associated with the stability of the simulated case. Therefore, MTI performs higher stability and less limitation.

3. In terms of error analysis, the errors of ITI only depend on the delay introduced by the parallel algorithm, which are smaller than the errors of TLI.

4. The errors of TLI are dependent on the associated capacitor of TLI and the equivalent admittance of the subsystem from the interface.

5. The errors of the MTI are convergent and much smaller than the previous two.

Through the proposed theorems and methods, the accuracy and stability of the multi-rate parallel simulation of DC grids are able to be evaluated conveniently. Multi-rate simulation has been performed to analyze the practical project, Zhoushan MTDC in China, which presents high speed and accuracy. The suitable multi-rate simulation algorithm can be applied in the analysis of DC grids to achieve fast and accurate simulation results."

The literature survey (subsection 2 in the revised introduction section) in incomplete. It should include related articles about DC power system analysis methods [1][2][3], parallel/distributed methods to deal with DC power networks [4], and also the stability analysis of large scale power systems [5] Authors need to review the mentioned articles carefully in the literature survey section. [1]. "Determination of the minimum-variance unbiased estimator for DC power-flow estimation." IECON 2014-40th Annual Conference of the IEEE Industrial Electronics Society. IEEE, 2014. [2] . "Error Detection of DC Power Flow Using State Estimation." Smart Grids: Security and Privacy Issues. Springer

International Publishing, 2017. 31-51. [3] "Sparsity-Based Error Detection in DC Power Flow State Estimation," IEEE International Electro/Information Technology Conference (EIT 2016), North Dakota, 2016. [4] "Distributed security constrained economic dispatch." Smart Grid Technologies-Asia (ISGT ASIA), 2015 IEEE Innovative. IEEE, 2015. [5] Vahdati, Pouya Mahdavipour, et al. "Hopf Bifurcation Control of Power Systems Nonlinear Dynamics Via a Dynamic State Feedback Controller--Part I: Theory and Modelling." IEEE Transactions on Power Systems (2016).

According to your constructive suggestion, the section of Literature review has been revised. References of the DC power flow, stability analysis of large-scale power system containing DC grids, the parallel DC network control have been included in the section 1.2 Literature review.

"DC grids, as an emerging technology, attract extensive studies. In [13], two multi-terminal DC modelling are studied in DC power flow using the Newton method. However, the operation modes of DC converters are too simple to present the practical situation. In [14], more general and detailed multi-terminal DC modelling in the sequential AC/DC power flow algorithm is proposed considering the power losses of the converters. The DC power flow method is simpler and faster than the Newton method. In [15, 16], a state estimation approach for linear problems is utilized in order to estimate the DC power flow. In [17], to remove the measure error, the sparse-based error detection technology is used to obtain the accurate DC power flow results. To manage DC network power, the distributed power dispatch method is proposed to replace the original centralized manner, which can greatly reduce the computation burden [18].

The transient study is another important aspect for large-scale power system containing DC grids. [19] proposed the MTDC modeling including DC lines, converters and DC controllers for transient study. In [20], the saturation of a generator is considered in the transient studies to investigate the bifurcation issues.

Electromagnetic simulation is still served as a major method for DC grid analysis [21]. The transient issues in DC grids, such as the DC controllers and IGBTs, belong to small time-scales, which can only be simulated using electromagnetic programs. Multi-rate parallel simulation is a suitable technology to analyze the DC grids and the interaction between a DC grid and a large-scale power system. The singular perturbation method is used to solve fast-slow systems [22]. However this method is not suitable for power electronics devices of which both fast and slow dynamics must be investigated, because this method uses asymptotic solution which neglects fast transients of the systems.

In order to investigate the fast transient of DC grids, there are three major algorithms to perform the parallel computation."

The following references are added:

"[13] X. Zhang, "Multiterminal voltage-sourced converter-based HVDC models for power flow analysis," IEEE Trans. Power Syst., vol. 19, no. 4, pp. 1877-1884, Nov., 2004.

[14] J. Beerten, S. Cole, and R. Belmans, "A sequential AC/DC power flow algorithm for networks containing Multi-terminal VSC HVDC systems," in 2010 IEEE Power and Energy Society General Meeting, 2010, pp. 1-7.

[15] M. Amini, A. I. Sarwat, S. S. Iyengar, and I. Guvenc, "Determination of the minimum-variance unbiased estimator for DC power-flow estimation," in IECON 2014 - 40th Annual Conference of the IEEE Industrial Electronics Society, 2014, pp. 114-118.

[16] K. G. Boroojeni, M. Hadi Amini, and S. S. Iyengar, "Error Detection of DC Power Flow

Using State Estimation," Smart Grids: Security and Privacy Issues, pp. 31-51, Cham: Springer International Publishing, 2017.

[17] M. H. Amini, M. Rahmani, K. G. Boroojeni, G. Atia, S. S. Iyengar, and O. Karabasoglu, "Sparsity-based error detection in DC power flow state estimation," in 2016 IEEE International Conference on Electro Information Technology (EIT), 2016, pp. 0263-0268.

[18] M. H. Amini, R. Jaddivada, S. Mishra, and O. Karabasoglu, "Distributed security constrained economic dispatch," in 2015 IEEE Innovative Smart Grid Technologies - Asia (ISGT ASIA), 2015, pp. 1-6.

[19] S. Lefebvre, W. K. Wong, J. Reeve, M. Baker, and D. Chapman, “Considerations for modeling MTDC systems in transient stability programs,” IEEE Trans. Power Del., vol. 6, no. 1, pp. 397-404, 1991.

[20] P. Mahdavipour Vahdati, A. Kazemi, M. H. Amini, and L. Vanfretti, “Hopf Bifurcation Control of Power Systems Nonlinear Dynamics Via a Dynamic State Feedback Controller--Part I: Theory and Modelling,” IEEE Trans. Power Syst., vol. PP, no. 99, pp. 1-1, 2017.

[21] M. Saeedifard, M. Graovac, R. F. Dias, and R. Iravani, "DC power systems: Challenges and opportunities," in Power and Energy Society General Meeting, 2010 IEEE, 2010, pp. 1-7”

Systematic Evaluation for Multi-rate Simulation of DC Grids

Qing Mu[1], *Student Member, IEEE*, Jun Liang[1], *Senior Member, IEEE*, Xiaoxin Zhou[2], *Life Fellow IEEE*, Chuanyue Li[1], *Member, IEEE*, Yalou Li[2], *Member, IEEE*
Cardiff University, Cardiff, CF24 3AA, U.K.
[2] China Electric Power Research Institute, 15 Xiaoyingdonglu, Haidian District, Beijing, 100192, China

***Abstract*—With wide applications of power electronic devices in modern power systems, simulation using traditional electromechanical and electromagnetic tools suffers low speed and imprecision. Multi-rate methods can enhance efficiency of simulation by decreasing the scale of systems in small time-steps. However, the existing traditional methods for multi-rate simulation suffer the problems of instability and simulation errors. These have hindered the application of multi-rate simulation in power industry. Therefore theoretical evaluation on different multi-rate simulation methods is crucial to understand the feasibility and limitation of the methods, and to contribute to overcome the drawbacks of the traditional methods. In this paper, the multi-rate simulation performance based on two traditional technologies and a Modified Thevenin Interface are evaluated to provide an overall feasibility of multi-rate algorithms in the power simulation. The Modified Thevenin Interface is proposed to overcome the drawbacks in synchronization. Three theorems are proposed and proved for theoretically analyzing the stability of the simulation methods. Error analyses of the multi-rate methods are performed to identify the relationships between errors and simulation conditions. Besides, the accuracy and efficiency performance in a practical project of VSC-MTDC shows the feasibility and necessity by using multi-rate simulation. Through the theoretical analysis, the issues of stability and accuracy of multi-rate simulation for the DC grids have been better understood, based on which an improved simulation algorithm has been proposed to overcome these issues. Long-term system dynamics of large-scale systems containing DC grids and fast transients of HVDC converters can be investigated simultaneously with high speed and sufficient accuracy.**

***Index Terms*—Electromagnetic transient analysis, Power System Simulation, Parallel Algorithm, Multi-rate Interface, Different Rates, Multi-terminal VSC-HVDC**

The research leading to these results has received funding from the People Programme (Marie Curie Actions) of the European Union's Seventh Framework Programme FP7/2007-2013/ under REA grant agreement no. 317221, project title MEDOW, and from the Project supported by the National Science Foundation for Distinguished Young Scholars of China (Grant No. 51407164).

NOMENCLATURE

$\mathbf{A_{f/s}}$	Matrix A in the state-space modelling [A, B, C, D]
Acc	Accurate Results
$\mathbf{B_{f/s}}$	Matrix B in the state-space modelling [A, B, C, D]
C	Capacitor C in Fig.1(F)
$\mathbf{C_{f/s}}$	Matrix C in the state-space modelling [A, B, C, D]
C_{TLI}	Associated capacitor of the equivalent transmission line
$\mathbf{D_{f/s}}$	Matrix D in the state-space modelling [A, B, C, D]
$diag[0,\mathrm{I}_{n1}]$	Diagonal matrix with the dimension of n_1
e	Exponent
e_{vf}	Errors of voltages at the interface (p.u.)
F	Constant associated with the system parameters
$g_f()$	Function to solve the open circuit voltages in the fast subsystem
$G_{\mathrm{f}}(\mathrm{s})$	Transfer function of the equivalent impedance of the fast subsystem
$g_s()$	Function to solve the open circuit voltages in the slow subsystem
$G_{\mathrm{s}}(\mathrm{s})$	Transfer function of the equivalent impedance of the slow subsystem
h	Small time-step (μs)
H	Large time-step (μs)
I_f	Interface current source (A)
i_f	Injected current of the interface in the fast subsystem (A)
I_s	Interface current source (A)
i_s	Injected current of the interface in the slow subsystem (A)
ITI	Ideal Transform Interface
k	Step index in the simulation of the slow subsystem
K	Constant associated with the system parameters
L_1	Inductor L_1 in Fig.1 (H)
L_2	Inductor L_2 in Fig.1(H)
m	Times between H and h
MTI	Modified Thevenin Equivalent Interface
$R(m)$	Constant associated with m, the times between the large time-step and slow time-step
T	Simulation time instant in the slow subsystem (μs)
t	Simulation time instant in the fast subsystem (μs)
TLI	Transmission Line Interface
$U_{fAA'}$	Input variables of the interface sources in the state-space modelling of the fast subsystem
U_{fint}	Input variables of the equivalent internal sources in the state-space modelling of the fast subsystem
$U_{sAA'}$	Input variables of the interface sources in the state-space modelling of the slow subsystem
U_{sint}	Input variables of the equivalent internal sources in the state-space

	modelling of slow subsystem
$V_{eqf}(s)$	Transfer function of Thevinen equivalent voltage sources of the fast subsystem
$V_{eqs}(s)$	Transfer function of Thevinen equivalent voltage sources of the slow subsystem
V_f	Voltage source of the interface branch in the fast system (V)
v_f	Voltage at the interface in the fast subsystem (V)
$v_{f\text{-}Exp}$	Expected voltage at the interface
V_{fint}	Equivalent internal voltage sources in the fast subsystem
$v_{f\text{-}ITI}$	Voltages at the interface using the ITI interface
$v_{f\text{-}TLI}$	Voltages at the interface using the TLI interface
V_s	Voltage source of the source branch in the slow system (V)
v_s	Voltage at the interface in the slow subsystem (V)
V_{sint}	Equivalent internal voltage sources in the slow subsystem
X_f	State variables of the fast subsystem
X_s	State variables of the slow subsystem
$Y_{fAA'}$	Output variables of the interface in the state-space modelling of the fast subsystem
$Y_{sAA'}$	Output variables of the interface in the state-space modelling of the slow subsystem
Z_1	Characteristic impedance of the transmission line (Ω)
Z_f	Equivalent impedance of the interface branch in the fast system
Z_s	Equivalent impedance of the interface branch in the slow system
ρ	Spectral radius of a matrix
$\Phi(m)$	State transfer matrix of the entire coupled system within a large time-step
$\Phi'(m)$	State transfer matrix of the entire coupled system using the single rate
$\Phi_f(i)$	State transfer matrix of the fast subsystem in *i*th small time-step within one large time-step
$\Phi_{non\text{-}int}(m)$	State transfer matrix of the entire coupled system without interpolation within a large time-step
Φ_s	State transfer matrix of the slow subsystem within a large time-step
$\Phi_{xnon\text{-}int}(m)$	State transfer matrix of the fast system without interpolation within a large time-step
$\|\|\Phi(m)\|\|_p$	An arbitrary norm of the state transfer matrix of the entire coupled system

1. Introduction

1.1. Motivation

In order to achieve the 202020 targets, the share of the renewable energy will rise greatly in different EU members [1]. A DC grid is an emerging transmission technology, which can provide flexible control to interconnect various renewable energies. A "super grid" to connect most of European countries shows the ambition in offshore wind power integration[2]. Simultaneous simulation of power electronics based DC systems and associated AC systems is a critical requirement for studies of DC grids, such as protection, stability and AC/DC interaction [3]. However, current tools for power system simulation perform less efficiently in this simultaneous simulation. Electromechanical simulation can hardly perform the transient in DC grids due to its large time-steps, although they are suitable for large-scale AC power systems[4]. Electromagnetics transient programs are able to simulate the detailed response in DC grids with a small time-step, but the simulation for AC/DC integrated systems with a small time-step will experience dramatically long time [5, 6].

Parallel computation in Electromagnetics transient simulation has been used for power system simulation, using the same time-step and data exchanged every step [7]. A large-scale system can be partitioned into several sub-systems, each of which can run independently in a separate Central Processing Unit (CPU). Therefore, the total calculation time is only a portion of the original one. However, due to the limitation of data communication, CPU numbers can not be increased unlimitedly to speed up the simulation. Normally parallel computation for power system simulation uses 8-12 cores in a server or 4-6 cores in a PC [8]. An entire power system is too large to be simulated using the current parallel simulation technology with a single time step.

Different simulation rates can be used in parallel computation, which is called multi-rate parallel algorithm. Components of power system have their dynamics with different time constants naturally. Components in DC grids with small time constants, such as AC/DC converters, DC/DC transformers and DC breakers, must use small time-steps to capture precise responses, while the conventional AC elements, which have slow dynamics, can use a large time-step in order to make computation fast.[9].

Multi-rate parallel algorithms essentially divide a system into several subsystems, which are simulated with suitable time-steps, in order to improve simulation speed. Not only integrated AC/DC systems, but also industrial applications in thermal/electrical co-simulation [10, 11], mechanical /electrical system co-simulation [12] can benefit from these algorithms.

1.2. Literature survey

DC grids, as an emerging technology, attract extensive studies. In [13], two multi-terminal DC modelling are studied in DC power flow using the Newton method. However, the operation modes of DC converters are too simple to present the practical situation. In [14], more general and detailed multi-terminal DC modelling in the sequential AC/DC power flow algorithm is proposed considering the power losses of the converters. The DC power flow method is simpler and faster than the Newton method. In [15, 16], a state estimation approach for linear problems is utilized in order to estimate the DC power flow. In [17], to remove the measure error, the sparse-based error detection technology is used to obtain the accurate DC power flow results. To manage DC network power, the distributed power dispatch method is proposed to replace the original centralized manner, which can greatly reduce the computation burden [18].

The transient study is another important aspect for large-scale power system containing DC grids. [19] proposed the MTDC modeling including DC lines, converters and DC controllers for transient study. In [20], the saturation of a generator is considered in the transient studies to investigate the bifurcation issues.

Electromagnetic simulation is still served as a major method for DC grid analysis [21]. The transient issues in DC grids, such as the DC controllers and IGBTs, belong to small time-scales, which can only be simulated using electromagnetic programs. Multi-rate parallel simulation is a suitable technology to analyze the DC grids and the interaction between a DC grid and a large-scale power system. The singular perturbation method is used to solve fast-slow systems [22]. However this method is not suitable for power

electronics devices of which both fast and slow dynamics must be investigated, because this method uses asymptotic solution which neglects fast transients of the systems.

In order to investigate the fast transient of DC grids, there are three major algorithms to perform the parallel computation, which can be extended to multi-rate simulations, the Ideal Transform Interface (ITI) [23], the Transmission Line Interface (TLI) [7, 24]and the Thevenin equivalent interface [25, 26].

There are concerns over instability and errors of the existing parallel methodologies for multi-rate simulation [23], which could limit the application for simulation of DC grids.

1.3. Contribution

This paper is to provide the systematic evaluation of the multi-rate simulation methods and investigate the stability and accuracy. The major contributions are listed as below:

1. An improved multi-rate method based on the Thevenin equivalent circuit, named Modified Thevenin Equivalent Interface (MTI), is proposed to overcome the issues of synchronization the in multi-rate simulation.

2. Three theorems have been proposed and proved to illustrate the stability characteristics of ITI, TLI and MTI.

3. The simulation errors using ITI, TLI and MTI have been analytically evaluated and the factors of these errors have been obtained.

4. The systematical analysis and comparisons of ITI, TLI and MTI have been performed.in terms of stability and accuracy.

1.4. Structure of paper

. The rest of this paper is organized as follows. In Section II, the multi-rate simulation method ITI and TLI is presented, while an improved multi-rate method based on the Thevenin equivalent circuit, named Modified Thevenin Equivalent Interface (MTI), is proposed to make it more suitable for DC grid simulation. Section III presents the analytical evaluation of the stability of three multi-rate simulation method. In Section IV, the analytical evaluation of the simulation errors of these multi-rate simulation methods is evaluated analytically. Section V presents a simulation study of different multi-rate simulation using the practical five-terminal MTDC as the test cases. Section V concludes the paper.

2. Multi-rate Simulation Methods

2.1. Ideal Transform Interface (ITI)

A simple circuit, as shown in Fig.1, is used for analyzing multi-rate simulation algorithms.

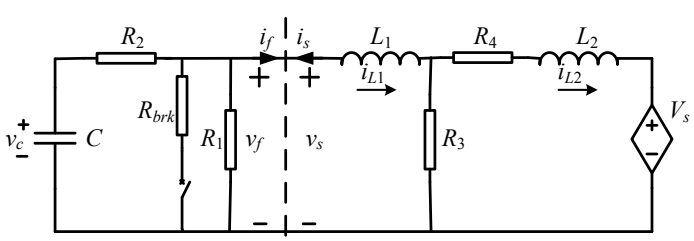

Fig. 1 Example System.

When the ideal transform interface is used [23]. The original circuit can be partitioned into two subsystems, fast and slow systems, as shown in Fig.2.

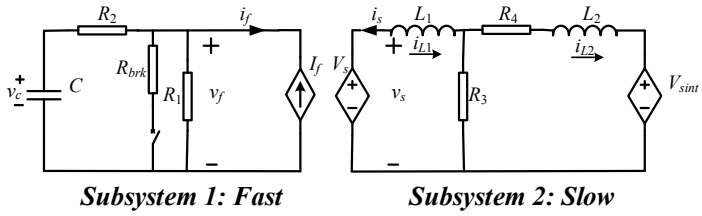

Fig. 2 ITI interface method.

The interface current source, I_f, is equal to the injected current of Subsystem 2, i_s. The interface voltage source V_s is equal to the voltage of the current source in Subsystem 1, v_f.

The subsystems are simulated with a small time-step, h, and a large time-step, $H=mh$, respectively. Data from a slow system to a fast system between different subsystems use the interpolation, and data from the fast system to the slow system is through a zero-order holder [27].

The formula for I_f and V_s will be achieved as:

$$\begin{cases} V_s(T+H)=v_f(T) \\ I_f(t)=\dfrac{H+T-t}{H}i_s(T-H)+\dfrac{t-T}{H}i_s(T) \end{cases} \tag{1}$$

where T is the simulation time instant in the slow system, and t is in the fast system, which is within the interval $[T, T+H]$.

2.2. Transmission Line Interface (TLI)

The transmission line interface is a widely applied method of parallel computation in AC systems [23, 24]. When there is no real transmission line in some areas of a power system, an inductor is introduced as an equivalent transmission line to decouple the system.

The original circuit in Fig.1 is partitioned into two subsystems with an equivalent transmission line, which utilizes L_1, as shown in Fig.3.

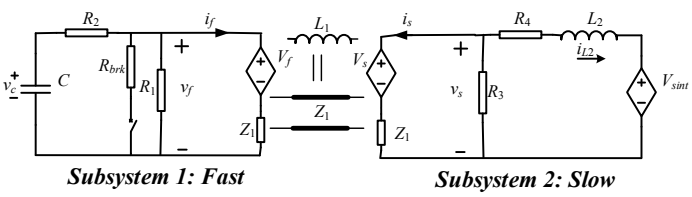

Fig. 3 TLI interface method.

The source branches, V_f, V_s and Z_1, represent the equivalent circuits of TLI terminals. Z_1 is the characteristic impedance of the transmission line, which is $2L_1/H$ in this example.

Similarly, interpolation is used for data from the slow system to the fast system, and a zero order hold is used from the fast to slow system. The decoupling equations are obtained:

$$\begin{cases} V_s(T+H)=V_f(T)+2i_f(T)Z_1 \\ V_f(t)=\dfrac{H+T-t}{H}(V_s(T-H)+2i_s(T-H)Z_1)+\dfrac{t-T}{H}(V_s(T)+2i_s(T)Z_1) \end{cases} \tag{2}$$

2.3. Modified Thevenin Equivalent Interface (MTI)

The ITI and the TLI have induced the latency to realize decoupling, which causes errors of node voltages and currents between the two sides of the interface.

The Thevenin equivalent circuit interface can alleviate these errors [10, 11], as shown in Fig.4.

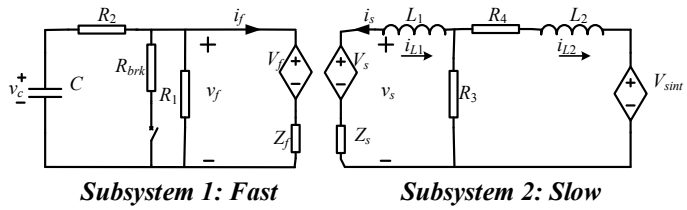

Fig. 4 MTI interface method.

V_f, V_s Z_s, and Z_f represent Thevenin equivalent circuits of the interface [25]. The Thevenin equivalent circuit method is commonly used in single rate simulation, where the interface equations are:

$$\begin{cases} V_s(t+h)=g_f(X_f(t)) \\ V_f(t+H)=g_s(X_s(t),V_{\sin t}(T)) \end{cases} \tag{3}$$

where X_f represents state variables in the fast subsystem, e.g. v_c in this case; X_s represents state variables in the slow subsystem, i_{L1} and i_{L2} in this case; g_f and g_s are the functions to solve the open circuit voltages in the subsystems.

However, due to different rates, the slow subsystem requires the $V_s(t+H)$, to calculate results for the next step, $t+H$, at the time of t. Obviously, $V_s(t+H) \neq V_s(t+h)$. There is the same challenge for calculating V_f.

Traditional Thevenin equivalent interfaces assume that the mean between $V_s(t)$ and $V_s(t+H)$ is approximately equal to $V_s(t+H)$ or $V_s(t+h)$. Then, $V_s(t+H)$ is substituted by the average value. But the existed issue on the accuracy and convergence should still be solved [28].

To surmount these obstacles in achieving the synchronization, an improvement proposed in this paper is to select proper history values to replace these state variables.

When the simulation goes to the time of t, the simulation in the subsystem with a small time step continues, however, for the large time step subsystem, the simulation will come back to the time of $t+h-H$ and achieve an integration of H to get the result of $t+h$. In this case, $V_s(t+h)$ is only required. A proper history time, $t+h-H$, is selected to make the slow subsystem compliant to the Thevenin equivalent source, $V_s(t+h)$.

Synchronization is thus achieved using accurate calculation based on the history value to avoid prediction which could cause unexpected errors and instability.

Rewriting (3), the decoupling equation will be obtained:

$$\begin{cases} V_s(t+h)=g_f(X_f(t)) \\ V_f(t+h)=\dfrac{t-T+h}{H}g_s(X_s(T),V_{\sin t}(t))+\dfrac{T+H-t-h}{H}g_s(X_s(T+H),V_{\sin t}(T+H)) \end{cases} \tag{4}$$

The MTI algorithm can decouple a system at any electrical nodes without losing the accuracy and stability. Therefore, subsystems with converters, e.g. wind generators, FACTS and more complicated DC grids, can be separated and run with different time-steps.

3. Stability Analysis

As illustrated in Fig.5, a network can be partitioned into two sub-networks, interconnected to each other, through an interface, *AA'*. Sub-networks with fast dynamics and slow dynamics are represented by the subscript, *f* or *s*, respectively.

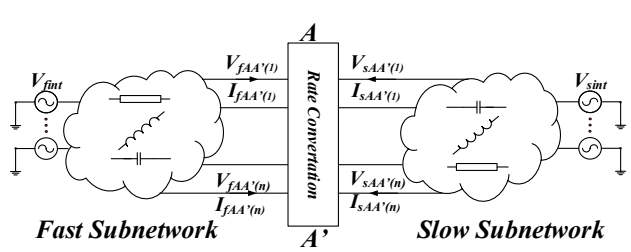

Fig. 5 Partition system for multi-rate simulation.

The state space of two sub-networks are given in (5) and (6):

$$\begin{cases}\dot{X}_f = A_f X_f + \left[B_{\text{fint}}\ B_{fAA'}\right]\left[U_{\text{fint}}\ U_{fAA'}\right]^T \\ Y_{fAA'} = C_f X_f + \left[D_{\text{fint}}\ D_{fAA'}\right]\left[U_{\text{fint}}\ U_{fAA'}\right]^T\end{cases} \tag{5}$$

$$\begin{cases}\dot{X}_s = A_s X_s + \left[B_{\text{sint}}\ B_{sAA'}\right]\left[U_{\text{sint}}\ U_{sAA'}\right]^T \\ Y_{sAA'} = C_s X_s + \left[D_{\text{sint}}\ D_{sAA'}\right]\left[U_{\text{sint}}\ U_{sAA'}\right]^T\end{cases} \tag{6}$$

where $U_{fint}=V_{fint}$ and $U_{sint}=V_{sint}$ are the input variables of each sub-network. $U_{fAA'}$ and $U_{sAA'}$ are the input variables from the interface. $Y_{fAA'}$ and $Y_{sAA'}$ represent output variables of subsystems.

By using the Backward Euler, the discrete type of equation (5) and (6) are obtained in (7) and (8),

$$\begin{cases} X_f(mk+1) = (I-hA_f)^{-1} X_f(mk) + (I-hA_f)^{-1} h\left[B_{f\text{int}}\ B_{fAA'}\right]\left[U_{f\text{int}}(mk+1)\ U_{fAA'}(mk+1)\right]^T \\ Y_{fAA'}(mk+1) = C_f X_f(mk+1) + \left[D_{f\text{int}}\ D_{fAA'}\right]\left[U_{f\text{int}}(mk+1)\ U_{fAA'}(mk+1)\right]^T\end{cases} \tag{7}$$

$$\begin{cases} X_s(mk+m) = (I-mhA_s)^{-1} X_s(mk) + (I-mhA_s)^{-1} mh\left[B_{\text{sint}}\ B_{sAA'}\right]\left[U_{\text{sint}}(mk+m)\ U_{sAA'}(mk+m)\right]^T \\ Y_{sAA'}(mk+m) = C_s X_s(mk+m) + \left[D_{\text{sint}}\ D_{sAA'}\right]\left[U_{\text{sint}}(mk+m)\ U_{sAA'}(mk+m)\right]^T\end{cases} \tag{8}$$

in which, k represents steps in the simulation.

For the stability analysis, the input variables inside each sub-network can be set as 0, which means U_{fint} and U_{sint} are 0.

The stability of integration algorithms indicates whether or not errors will be accumulated during the integration [29], no matter if the system under study is stable or not. Stability is an important index of simulation accuracy, which can be determined through the system norms [30].

3.1. Stability Analysis for ITI

3.1.1 State Transfer Matrix for ITI

Assuming that the input variables in the fast subsystem, $U_{fAA'}$, are the injected current through the interface, $I_{fAA'}$, and the input variables in the slow subsystem, $U_{sAA'}$, is the voltages on the interface, $V_{sAA'}$. The output variables, $Y_{fAA'}$ and $Y_{sAA'}$, are the $V_{fAA'}$ and $I_{sAA'}$, respectively. To be simplified, $V_{sAA'}$ is denoted as V_s and $I_{fAA'}$ is denoted as I_f.

According to Fig.5, rewrite the decoupling equation (1) in the forms of discretion,

$$\begin{cases} V_s(mk) = V_{fAA'}(mk-m) \\ I_f(mk+i) = \dfrac{m-i}{m} I_{sAA'}(mk-m) + \dfrac{i}{m} I_{sAA'}(mk)\end{cases} \tag{9}$$

where i represent the ith steps between mk and $m(k+1)$.

Considering the decoupling equation (9), the discrete equation can be rewritten:

$$\begin{cases} X_f(mk+i) = (I-hA_f)^{-1} X_f(mk+i-1) + (I-hA_f)^{-1} hB_{fAA'} \\ \qquad\qquad \left(\dfrac{m-i}{m} I_f(mk) + \dfrac{i}{m}(C_s X_s(mk) + D_{sAA'} V_s(mk))\right) \\ V_s(mk+i) = C_f X_f(mk-m+i) + D_{fAA'}\left(\dfrac{m-i}{m} I_f(mk-m) + \dfrac{i}{m} I_f(mk)\right)\end{cases} \tag{10}$$

$$\begin{cases} X_s(mk+m) = (I-mhA_s)^{-1} X_s(mk) + (I-mhA_s)^{-1} mhB_{sAA'} \\ \qquad\qquad (C_f X_f(mk) + D_{fAA'} I_f(mk)) \\ I_f(mk+m) = C_s X_s(mk) + D_{sAA'} V_s(mk)\end{cases} \tag{11}$$

There are m steps of simulation with a small time-step for the fast system, whose state transfer equation for the m th calculation is shown in (12), and one step of simulation with a large time-step for the slow system, whose state transfer equation is shown in (14).

$$\left[X_f(k+1)\,X_s(k)\,I_f(k)\,V_s(k)\right]'=\prod_{i=1}^{m}\Phi_f(i)\left[X_f(k)\,X_s(k)\,I_f(k)\,V_s(k)\right]' \tag{12}$$

where the $\Phi_f(i)$ represents the transfer matrix in the ith small step within one large time-step, as below:

$$\Phi_f(i)=\begin{bmatrix} A_{11} & A_{12} & A_{13} & A_{14} \\ 0 & & I & \end{bmatrix} \tag{13}$$

where $A_{11}=(I-hA_f)^{-1}A_{12}=(I-hA_f)^{-1}hB_{fAA'}i/mC_s$ $A_{13}=(I-hA_f)^{-1}hB_{fAA'}(m-i)/m$ and $A_{14}=(I-hA_f)^{-1}hB_{fAA'}i/mD_{sAA'}$.

$$\left[X_f(k)\,X_s(k+1)\,I_f(k+1)\,V_s(k+1)\right]'=\Phi_s\left[X_f(k)\,X_s(k)\,I_f(k)\,V_s(k)\right]' \tag{14}$$

where Φ_s represents the transfer matrix of the slow system as below:

$$\Phi_s=\begin{bmatrix} I & 0 & 0 & 0 \\ A_{21} & A_{22} & A_{23} & 0 \\ 0 & C_s & 0 & D_{sAA'} \\ C_f & 0 & D_{fAA'} & 0 \end{bmatrix} \tag{15}$$

where $A_{21}=(I-mhA_s)^{-1}mhB_{sAA'}\mathrm{C_f}$ $A_{22}=(I-mhA_s)^{-1}$ $A_{23}=(I-mhA_s)^{-1}mhB_{sAA'}D_{fAA'}$.

Combine (12) and (14), the transfer state equations of whole system can be obtained:

$$\left[X_f(k+1)\,X_s(k+1)\,I_f(k+1)\,V_s(k+1)\right]'=\Phi(m)\left[X_f(k)\,X_s(k)\,I_f(k)\,V_s(k)\right]' \tag{16}$$

where $\Phi(m)$ represents the state transfer as below:

$$\Phi(m)=diag[0,\mathrm{I}_{n1}]\Phi_s+diag[\mathrm{I}_{n2},0]\prod_{i=1}^{m}\Phi_f(i) \tag{17}$$

And $diag[0,\mathrm{I}_{n1}]$ represents a diagonal matrix, n_1 is the summary of the dimension of X_s, I_f and V_s, and n_2 is the dimension of the dimension of X_f.

This matrix, $\Phi(m)$, fully represents the dynamics of this multi-rate simulation and is thus used to evaluate the algorithm stability.

3.1.2 Stability Theorem for Multi-rate without Interpolation

The norm of state transfer matrix determines the algorithm stability. The criteria [31] is that a system is stable, when

$$\rho(\Phi(m))\le\|\Phi(m)\|_{\mathrm{p}}\le 1 \tag{18}$$

where $||\Phi(m)||_p$ represents an arbitrary norm, ρ represents the spectral radius of a matrix.

Theorem 1:

If simulation of ITI using a single rate is stable, and the divided fast and slow subsystems are also asymptotically stable, then the multi-rate simulation algorithm without interpolation is stable as long as all the multiple rates are not larger than the single rate.

Proof:

Discretizing (5) and (6) in the large time-step, $H=mh$, and combining the decoupling equation (9) when $i=m=1$, a new state transfer function can be obtained:

$$\begin{cases} X_f(k+1)=(I-HA_f)^{-1}X_f(k)+(I-HA_f)^{-1}HB_{fAA'}(C_sX_s(k)+D_{sAA'}V_s(k)) \\ V_s(k+1)=C_fX_f(k)+D_{fAA'}I_f(k) \end{cases} \tag{19}$$

$$\begin{cases} X_s(k+1)=(I-HA_s)^{-1}X_s(k)+(I-HA_s)^{-1}HB_{sAA'}(C_fX_f(k)+D_{fAA'}I_f(k)) \\ I_f(k+1)=C_sX_s(k)+D_{sAA'}V_s(k) \end{cases} \tag{20}$$

Then, the following state transfer function can be derived,

$$\left[X_f(k+1)\,X_s(k+1)\,I_f(k+1)\,V_s(k+1)\right]'=\Phi'(m)\left[X_f(k)\,X_s(k)\,I_f(k)\,V_s(k)\right]'$$

where $\Phi'(m)$ represents the state transfer, whose norm should be less than 1, as below:

$$\Phi'(m)=\begin{bmatrix} A_{11}' & A_{12}' & A_{13}' & A_{14}' \\ A_{21} & A_{22} & A_{23} & 0 \\ 0 & C_s & 0 & D_{sAA'} \\ C_f & 0 & D_{fAA'} & 0 \end{bmatrix}$$
$$\|\Phi'(m)\|<1 \tag{21}$$

where A_{21}, A_{22}, A_{23} is the same as (15) and A_{11}', A_{12}', A_{13}', A_{14}' is as below.

$A_{11}'=(I-HA_f)^{-1}$ $A_{12}'=(I-HA_f)^{-1}HB_{fAA'}C_s$ $A_{13}'=0$ $A_{14}'=(I-HA_f)^{-1}HB_{fAA'}D_{sAA'}$

Find a matrix $\Phi_x'(m)$ to make $\Phi'(m)=\Phi_x'(m)\,\Phi_s$, then

$\Phi_x'(m)$ is as below:

$$\Phi_x'(m)=\begin{bmatrix} A_{x11}' & A_{x12}' & A_{x13}' & A_{x14}' \\ 0 & & I & \end{bmatrix} \tag{22}$$

where $A_{x11}'=(I-HA_f)^{-1}$.

When the data exchange for the multi-rate simulation without interpolating and smoothing process, rewrite the decoupling equation (9) in the forms of discretion.

$$\begin{cases} V_s(mk)=V_{fAA'}(mk-m) \\ I_f(mk+i)=I_{sAA'}(mk) \end{cases} \tag{23}$$

Using the similar derivation from (10) to (16), the state transfer, $\Phi_{non\text{-}int}(m)$, matrix can be obtained:

$$\Phi_{non-\text{int}}(m)=\begin{bmatrix} A_{11}^* & A_{12}^* & A_{13}^* & A_{14}^* \\ A_{21} & A_{22} & A_{23} & 0 \\ 0 & C_s & 0 & D_{sAA'} \\ C_f & 0 & D_{fAA'} & 0 \end{bmatrix} \tag{24}$$

where A_{21}, A_{22}, A_{23} is the same as (15) and A_{11}*, A_{12}*, A_{13}*, A_{14}* is as below,

$A_{11}^*=(I-hA_f)^{-m}$ $A_{12}^*=\sum_{i=1}^{m}((1-hA_f)^{-1})^{m-i+1}hB_{fAA'}C_s$

$A_{13}^*=0$ $A_{14}^*=\sum_{i=1}^{m}((1-hA_f)^{-1})^{m-i+1}hB_{fAA'}D_{sAA'}$

Find a matrix $\Phi_{xnon\text{-}int}(m)$ to make $\Phi_{non\text{-}int}(m)=\Phi_{xnon\text{-}int}(m)\,\Phi_s$, then $\Phi_{xnon\text{-}int}(m)$ is as below:

$$\Phi_{xnon-\text{int}}(\text{m})=\begin{bmatrix} A_{x11}^* & A_{x12}^* & A_{x13}^* & A_{x14}^* \\ 0 & & I & \end{bmatrix} \tag{25}$$

where $A_{x11}^*=(I-hA_f)^{-m}$

Comparing with the norm of A_{x11}* and A_{x11}', when norm of A_f is less than 1, which is the requirement of the stability in the fast subsystem, the norm of A_{x11}* is less than the norm of A_{x11}'. Also, the norm of A_{x11}* and A_{x11}' will determine the norm of $\Phi_{xnon\text{-}int}(m)$ and $\Phi_x'(m)$, respectively.

Then, an inequality can be obtained:

$$\|\Phi_{xnon-\text{int}}(m)\|<\|\Phi_x'(m)\| \tag{26}$$

Because $\Phi'(m)=\Phi_x'(m)\Phi_s$ and $\Phi_{non\text{-}int}(m)=\Phi_{xnon\text{-}int}(m)\Phi_s$, then the norm of $\Phi_{non\text{-}int}(m)$ can be achieved as:

$$\|\Phi_{non-\text{int}}(m)\|<\|\Phi'(m)\|<1 \tag{27}$$

This proves the multi-rate integration method without interpolation is stable and the **Theorem 1** is proved.

3.1.3 Stability Analysis for Multi-rate with Interpolation

The transfer matrix $\Phi(m)$ in (16) can be transferred to $\Phi(m)=\Phi_x(m)\,\Phi_s$, then $\Phi_x(m)$ is given as below:

$$\Phi_x(\text{m})=\begin{bmatrix} A_{x11} & A_{x12} & A_{x13} & A_{x14} \\ 0 & & I & \end{bmatrix} \tag{28}$$

where $A_{x11}=((I-hA_f)^{-1})^{\text{m}}-\text{C}_{\text{f}}\sum_{i=1}^{m}((1-hA_f)^{-1})^{m-i+1}hB_{fAA'}\frac{m-i}{m}D_{fAA'}^{-1}$

Similarly to the previous section, if the norms of A_{x11} are less than the norms of A_{x11}', the norms of $\Phi(m)$ can be found less than $\Phi'(m)$ and less than 1, which means that the multi-rate integration method with interpolation is stable.

However, the norms of A_{x11} can not be directly proved to be less than A_{x11}', some tools can help to calculate the norm of A_{x11} to evaluate the stability of the multi-rate simulation with interpolation in the cases. Normally, it is stable as well.

In conclusion, with a large time-step and a small time-step, the stability of the multi-rate algorithm of ITI is better than the parallel computation of ITI with the single rate of the same large time-step. However, [23] indicates that the parallel computation of ITI with a single rate hardly keeps the stability, because of the artificial induced latency.

3.2. Stability Analysis for TLI

3.2.1 State Transfer Matrix for TLI

As illustrated in Fig.3, V_f and V_s of the equivalent source branches of TLI are the input variables, $U_{fAA'}$ and $U_{sAA'}$, in fast and slow subsystems. The output variables $Y_{fAA'}$ and $Y_{sAA'}$ represent the $V(mk-m)+2i(mk-m)Z_1$, denoted as Y_f and Y_s for simplification.

Rewrite the equation (2) in the forms of discretion,

$$\begin{cases} V_f(mk+i)=\dfrac{m-i}{m}Y_s(mk-m)+\dfrac{i}{m}Y_s(mk) \\ V_s(mk)=Y_f(mk-m) \end{cases} \tag{29}$$

Considering the decoupling equation (29), using the system equation (7) and (8), the discrete equations can be achieved. In fact, they are as same as (10), (11), except that V_f replaces I_f.

Similarly, deriving from (12) to (16), the state transfer matrix $\Phi(m)$ can be obtained, as below, to evaluate the stability of the TLI.

$$\Phi_{TLI}(m)=\begin{bmatrix} A_{11} & A_{12} & A_{13} & A_{14} \\ A_{21} & A_{22} & A_{23} & 0 \\ 0 & C_s & 0 & D_{sAA'} \\ C_f & 0 & D_{fAA'} & 0 \end{bmatrix} \tag{30}$$

where A_{21}, A_{22}, A_{23} is the same as (15) and A_{11}, A_{12}, A_{13}, A_{14} is,

$$A_{11}=(I-hA_f)^{-m}\ A_{12}=\sum_{i=1}^{m}((1-hA_f)^{-1})^{m-i+1}h\frac{i}{m}B_{fAA'}\mathrm{C}_s$$

$$A_{13}=\sum_{i=1}^{m}((1-hA_f)^{-1})^{m-i+1}h\frac{m-i}{m}B_{fAA'}A_{14}=\sum_{i=1}^{m}((1-hA_f)^{-1})^{m-i+1}h\frac{i}{m}B_{fAA'}D_{sAA'}$$

3.2.2 Stability Analysis for Multi-rate Algorithm

Theorem 2:

If the simulation of TLI with a single rate is stable, and the divided fast and slow subsystems are also asymptotically stable, then the multi-rate simulation algorithm without interpolation is stable as long as all the multiple rates are not larger than the single rate.

The assumption of this theorem includes that:

- A system is divided into subsystems;
- Stable simulation can be achieved for the subsystems connected through TLI interface using the same time-steps for all subsystems, called a single rate, H. This means that the state transfer matrix in an equation, similar to (21), has the norms less than 1;
- Each subsystem is asymptotically stable, which means that the A11 and A22 in (30) have norms less than 1;
- Different simulation time-steps, which are not larger than the single rate H, are used for subsystems. Fast subsystems have small time-steps and slow subsystems have relatively large time-steps.

When the above assumptions are met, stable simulation can be achieved for the fast and slow subsystems connected through TLI.

This theorem can be proved using the similar procedure from (19) to (27).

For a similar matrix A_{x11} in (31) can be achieved for the multi-rate TLI with interpolation in order to compare with A_{11} in (30).

$$A_{x11}=((I-hA_f)^{-1})^{\mathrm{m}}-\mathrm{C_f}\sum_{i=1}^{m}((1-hA_f)^{-1})^{m-i+1}hB_{fAA'}\frac{m-i}{m}D_{fAA'}{}^{-1} \tag{31}$$

Rewrite (31):

$$A_{x11}=((I-hA_f)^{-1})^{m}(\mathrm{I}-\mathrm{C_f}(1-hA_f)^{-1}hB_{fAA'}\sum_{i=1}^{m}((1-hA_f)^{-1})^{-i}\frac{m-i}{m}D_{fAA'}{}^{-1}) \tag{32}$$

Normally, the stability of multi-rate algorithm is usually met by calculating the norm of A_{x11}.

In conclusion, For TLI, the stability of the simulation with different rates depends on the stability of the simulation with the single rate of a large time-step. However, [23] indicates that simulation of the TLI with a single rate always keeps stability.

3.3. Stability Analysis for MTI

3.3.1 State Transfer Matrix for MTI

$U_{fAA'}$ and $U_{sAA'}$ represent the interface voltages at the two sides respectively. $Y_{fAA'}$ and $Y_{sAA'}$ represent the currents through the interface.

Rewrite the relationship of voltages and currents in the interface in the forms of discretion.

$$\begin{cases} U_{fAA'}(mk)=U_{sAA'}(mk) \\ Y_{fAA'}(mk)=-Y_{sAA'}(mk) \end{cases} \tag{33}$$

Using the system equations (7), (8) and (33) and removing the intermediate variables, $U_{fAA'}$, $U_{sAA'}$ and $Y_{fAA'}$ and $Y_{sAA'}$, the discrete equations can be rewritten:

$$\begin{cases} X_f(mk+i)=A_{ff}X_f(mk+i-1)+A_{fs}(\frac{m-i}{m}X_s(mk-m)+\frac{i}{m}X_s(mk)) \\ X_s(mk+m)=A_{sf}X_f(mk+m-1)+A_{ss}X_s(mk) \end{cases} \tag{34}$$

where $A_{ff}=A_{f\text{-}dis}-B_{fdis}\Delta C_f A_{f\text{-}dis}$, $A_{fs}=-B_{fdis}\Delta C_s A_{s\text{-}dis}$,

$A_{s\text{-}dis}=(I-mhA_s)^{-1}$, $A_{ss}=A_{s\text{-}dis}-B_{sdis}\Delta C_s A_{s\text{-}dis}$ $A_{sf}=-B_{sdis}\Delta C_f A_{f\text{-}dis}$,

$A_{f\text{-}dis}=(I-hA_f)^{-1}$, $B_{fdis}=(I-hA_f)^{-1}hB_{fAA'}$, $B_{sdis}=(I-mhA_s)^{-1}mhB_{sAA'}$

Similar, the procedure of multi-rate simulation is divided as *m-1* steps of simulation with a small time-step for the fast system, whose state transfer equation is shown in (35), and one step of simulation for the entire system, whose state transfer equation is shown in (37).

$$\begin{bmatrix} X_f(mk+i) \\ X_s(mk) \\ X_s(mk-m) \end{bmatrix}=\Phi_f(i)\begin{bmatrix} X_f(mk+i-1) \\ X_s(mk) \\ X_s(mk-m) \end{bmatrix} \tag{35}$$

where $\Phi_f(i)$ represents the transfer matrix in the *i*th step among a large time-step, as below:

$$\Phi_f(i)=\begin{bmatrix} A_{ff} & \frac{i}{m}A_{fs} & \frac{m-i}{m}A_{fs} \\ 0 & & I \end{bmatrix} \tag{36}$$

$$\begin{bmatrix} X_f(mk+m) \\ X_s(mk+m) \\ X_s(mk) \end{bmatrix}=\Phi_s\begin{bmatrix} X_f(mk+m-1) \\ X_s(mk) \\ X_s(mk-m) \end{bmatrix} \tag{37}$$

where Φ_s represents the transfer matrix of the slow system:

$$\Phi_s=\begin{bmatrix} A_{ff} & A_{fs} & 0 \\ A_{sf} & A_{ss} & 0 \\ 0 & I & 0 \end{bmatrix} \tag{38}$$

The whole system can be derived for its state transfer matrix, represented by $\Phi(m)$,

$$\Phi(m)=\Phi_s\prod_{i=1}^{m-1}\Phi_f(i) \tag{39}$$

3.3.2 Stability Analysis

Theorem 3:

If the original system is asymptotically stable, and the divided fast and slow subsystems are also asymptotically stable. Then simulation using proposed MTI algorithm is stable.

Proof:

Let A_{ff} and A_{ss} be the discrete state matrix of the fast system and the slow system respectively, the norm of A_{ff} and A_{ss} is less than 1, therefore according to (36), the norm of $\Phi_f(i)$ is less than 1.

Meanwhile, the state matrix of the original system can be obtained through eliminating the variable $U_{sAA'}$ and $Y_{sAA'}$, represented by A.

$$\begin{bmatrix} \dot{X}_f \\ \dot{X}_s \end{bmatrix} = \begin{bmatrix} A_f - B_{fAA'}(D_f+D_s)^{-1}C_f & -B_{fAA'}(D_f+D_s)^{-1}C_s \\ -B_{sAA'}(D_f+D_s)^{-1}C_f & A_s - B_{sAA'}(D_f+D_s)^{-1}C_s \end{bmatrix} \begin{bmatrix} X_f \\ X_s \end{bmatrix} \tag{40}$$

Also, suppose $A(m)$, which can be factorized as below.

$$A(m) = \begin{bmatrix} I & 0 \\ 0 & mI \end{bmatrix} A = \begin{bmatrix} A_f - B_{fAA'}(D_f+D_s)^{-1}C_f & -B_{fAA'}(D_f+D_s)^{-1}C_s \\ -mB_{sAA'}(D_f+D_s)^{-1}C_f & mA_s - mB_{sAA'}(D_f+D_s)^{-1}C_s \end{bmatrix} \tag{41}$$

$A(m)$ is used as the state matrix of a new system. Since the original system absolute stable, all eigenvalues of the A has the negative real part. Then, all eigenvalues of the $A(m)$ has the negative real part. It deduces that the new system is absolutely stable.

h is chosen as the unified time-step for this new system, the discretized state transfer matrix is obtained as below:

$$\begin{cases} X_f(k+1) = \left(A_{f-dis} - B_{fAA'-dis}\Delta C_f A_{f-dis}\right)X_f(k) \\ \qquad\qquad - B_{fAA'-dis}\Delta C_s A_{s-dis} X_s(k) \\ X_s(k+1) = -B_{sAA'-dis}\Delta C_f A_{f-dis} X_f(k) \\ \qquad\qquad + \left(A_{s-dis} - B_{sAA'-dis}\Delta C_s A_{s-dis}\right)X_s(k) \end{cases} \tag{42}$$

And $\Delta = (C_s B_{sAA'-dis} + D_{fAA'} + D_{sAA'} + C_f B_{fAA'-dis})^{-1}$

The state transfer matrix is Φ_{s11}, whose norms is less than 1.

$$\Phi_{s11} = \begin{bmatrix} A_{ff} & A_{fs} \\ A_{sf} & A_{ss} \end{bmatrix} \tag{43}$$

This matrix is found to be just the sub-matrix of Φ_s in (38). Thus the norms of Φ_s is less than 1.

Follow that,

$$\Phi(m) = \Phi_s \prod_{i=1}^{m-1} \Phi_f(i) < 1 \tag{44}$$

Hence, the MTI algorithm is stable as long as the original system is stable.

3.4. Stability Evaluation

In this part, the stability of the example system in Fig.1 will be studied to verify the proposed theorems of ITI, TLI and MTI.

The norm of the systems in both the multi-rate simulation and the single-rate simulation using large time-steps were calculated using the eigenvalue method for various circuit parameters, as shown in Fig.6-8. The comparison involves three interfaces. The dash line is the boundary of stability, as the legend of “ref”.

Considering ITI, the norms of the system in the single-rate simulation are always larger than the multi-rate simulation. This verifies the Theorem 1. Also, the multi-rate method of ITI is stable, as long as ITI parallel simulation with a single-rate is stable. However, although the original system is stable, ITI parallel simulation with a single-rate becomes unstable when the norms exceed the "ref" value, as shown in Fig.6(a) and 7(a). This is due to artificial time delay between subsystems [14].

Considering TLI, the norms of the system in the single-rate simulation are always larger than in the multi-rate simulation. This verifies the Theorem 2. In most cases, the TLI is stable. However, the transmission line can also reduce the stability of simulation, compared with lumped inductors.

Among three multi-rate method, the stability of MTI is always the most stable under all conditions. Because no simplification is required in the MTI, the stability of this method is just slightly lower than the original simulation, and higher than the previous two methods. This verifies the Theorem 3.

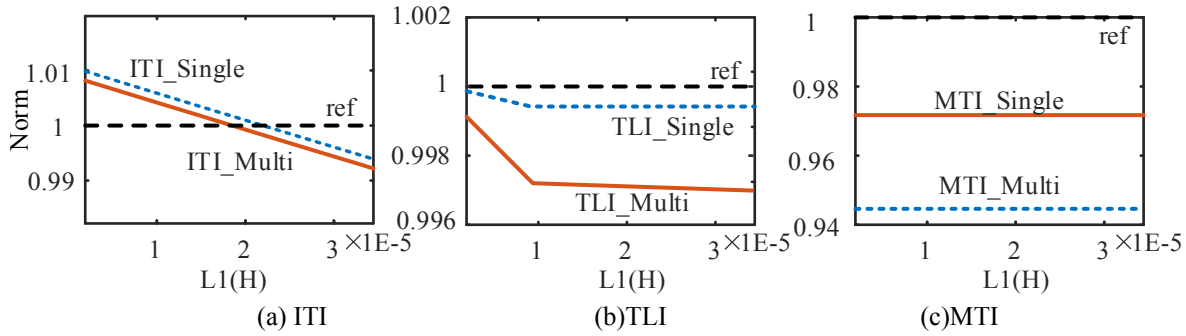

Fig. 6 Stability evaluation using various connected inductors.

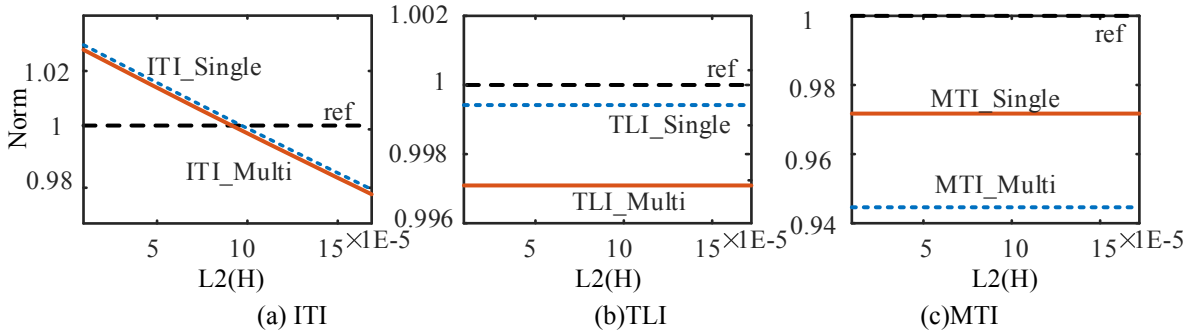

Fig. 7 Stability evaluation using various inductors L_2 in the network with a large time-step.

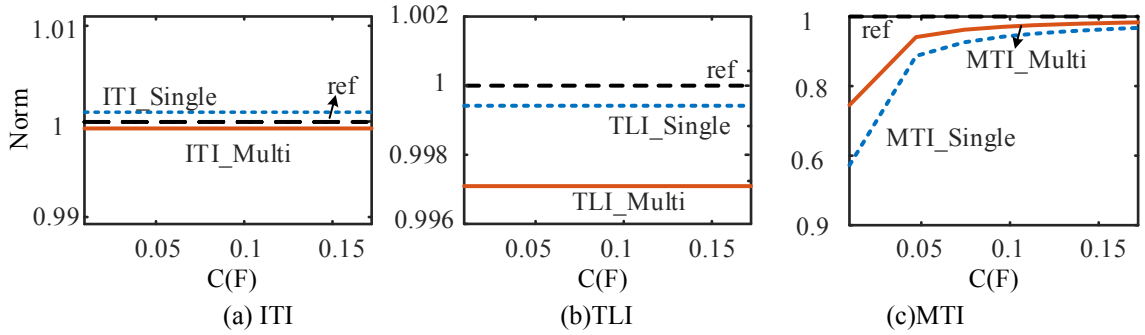

Fig. 8 Stability evaluation using various capacitors in the network with a small time-step.

4. Error Analysis

This section evaluates factors influencing errors of the multi-rate simulation. These include time-steps, interface inductor and parameters in both small and large time-step networks.

4.1. Decoupling Interface errors

For ITI, the equivalent circuit is shown in Fig.9 (a).

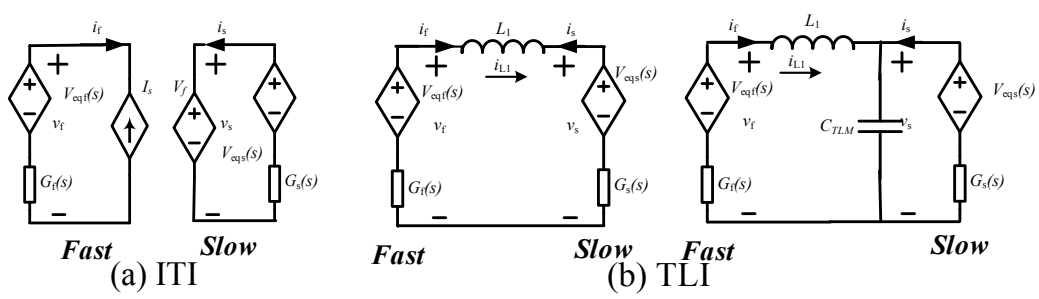

Fig. 9 Thevenin Equivalent Circuit.

where V_{eqs}(s) and V_{eqf}(s) represent the Thevinen equivalent sources of the subsystems, and G_s(s) and G_f(s) are the impedance in the equivalent sources.

Because there are the induced latency in ITI as below,

$$\begin{cases} I_s(s)=i_s(s)\mathrm{e}^{-Hs} \\ V_f(s)=v_f(s)\mathrm{e}^{-Hs} \end{cases} \tag{45}$$

The voltage, v_f, in the interface can be derived as below,

$$v_{f-ITI}=\frac{v_{eqs}(s)\mathrm{e}^{-Hs}G_f(s)}{G_s(s)+\mathrm{e}^{-2Hs}G_f(s)}+\frac{v_{eqf}(s)\mathrm{e}^{-Hs}G_s(s)}{G_s(s)\mathrm{e}^{-2Hs}+G_f(s)} \tag{46}$$

Alternatively, the expected result is as below,

$$v_{f-Exp}=\frac{v_{eqs}(s)G_f(s)}{G_s(s)+G_f(s)}+\frac{v_{eqf}(s)G_s(s)}{G_s(s)+G_f(s)} \tag{47}$$

The time-step H is always small, so that the e^{-2Hs} is close to 1, it can be assumed that

$$G_s(s)+\mathrm{e}^{-2Hs}G_f(s)=G_s(s)+G_f(s)=\mathrm{e}^{-2Hs}G_s(s)+G_f(s) \tag{48}$$

Therefore, the error can be obtained as below,

$$e_{v_f}=\left|\frac{v_{f-ITI}-v_{f-Exp}}{v_{f-Exp}}\right|=\left|\mathrm{e}^{-Hs}-1\right| \tag{49}$$

For TLI, an inductor is used as an equivalent transmission line. The difference between the original circuit and the circuit with a transmission line is shown in Fig.9 (b), where the associated capacitor of the equivalent transmission line is C_{TLI}, which is the can be obtained , $C_{\mathrm{TLI}}=H^2/L_1$.

The voltage in the interface for the original system and the circuit with TLI interface can be obtained:

$$v_{f-TLI}=\frac{v_{eqs}(s)(L_1s+G_f(s))+v_{eqf}(s)(G_s(s)+L_1s+L_1C_{TLI}s^2G_s(s))}{G_s(s)+L_1s+L_1C_{TLI}s^2G_s(s)+G_f(s)+G_s(s)G_f(s)sC_{TLI}} \tag{50}$$

$$v_{f-Exp}=\frac{v_{eqs}(s)(G_f(s)+\mathrm{L}_1\mathrm{s})}{G_s(s)+G_f(s)+\mathrm{L}_1\mathrm{s}}+\frac{v_{eqf}(s)(G_s(s)+\mathrm{L}_1\mathrm{s})}{G_s(s)+G_f(s)+\mathrm{L}_1\mathrm{s}} \tag{51}$$

Because the time-step H is very small, and the $L_1C_{\mathrm{TLI}}=H^2$ are close to 0,

$$\begin{aligned} &G_s(s)+L_1s+L_1C_{TLI}s^2G_s(s)=G_s(s)+\mathrm{L}_1\mathrm{s} \\ &G_s(s)+L_1s+L_1C_{TLI}s^2G_s(s)+G_f(s)+G_s(s)G_f(s)sC_{TLI} \\ &=G_s(s)+L_1s+G_f(s)+G_s(s)G_f(s)sC_{TLI} \end{aligned} \tag{52}$$

Therefore, the error can be obtained as below,

$$e_{v_f}=\left|\frac{v_{f-TLI}-v_{f-Exp}}{v_{f-Exp}}\right|=\left|\frac{G_s(s)G_f(s)sC_{TLI}}{G_s(s)+G_f(s)+L_1s+G_s(s)G_f(s)sC_{TLI}}\right| \tag{53}$$

The error is dependent on the associated capacitor, and the configuration of the internal circuits affects the error as well. Stability analysis indicates that the errors of the ITI and TLI can only be evaluated when the simulation is stable.

For the MTI, the external circuit is exactly represented using Thevenin equivalent circuit, and no artificial simplification is involved in the method. Therefore, errors of MTI are much smaller than the previous too.

Also, Errors evaluation can be obtained as below [32]:

$$e(kH)<\|R(m)\|KHe^{FHk}-\|R(m)\|KH \tag{54}$$

where $\|R(m)\|$ is a constant for a given m. K and F are constants, which can be calculated with the system parameters. k represents the kth steps in the simulation.

This indicates that the maximum simulation errors within a simulation stage are limited and can be reduced as long as H, the large time-step, is small enough. And also, along with the time constants of the subsystems increase, K and F may increase to enlarge the errors, but the detailed evaluation of K and F is still required.

4.2. Error Evaluation

The accuracy of the example system in Fig.1 will be studied to verify the theoretical analysis of errors of the ITI, TLI and MTI. The error evaluation for various conditions is illustrated in Fig.10 to 15. The dark lines represent simulation errors, while the grey line represents expected errors in theory for ITI and TLI, and as expected errors of MTI are exceedingly small, which are not shown in figures.

The results of increasing the large time-step are shown in Fig.10. The errors of ITI in Fig.10(a) increase due to the increased delay as proved in (49) and are approximately proportional to the increase in the large time-step. The trends of expected errors (ITI_Exp) and simulation errors (ITI) are the same, although there is about 20% difference between them. The errors of TLI in Fig.10(b) increase due to the increased associated capacitor, C_{TLI}, as proved in (53). They are large than ITI, and the expected errors (TLI_Exp) are coincide with the simulation ones (TLI). The errors of MTI in Fig.10(c) are much less than others, only being lower than 0.03%.

Increasing of a small time-step doesn't affect the errors, as shown in Fig.11, as the artificial delay of ITI and the associated capacitor of TLI are not increased. The simulation errors of ITI and TLI are close to their expected errors. Errors of MTI have no increment.

As shown in Fig.12, higher errors could be found for signals with higher frequency. s in formulas of errors, (49) and (53), is determined by the frequency. A little difference between the simulation errors and the expected error exists. Simulation errors of TLI increase with the same rate of expected errors. The errors of MTI increases, still being smaller than 0.01%.

Increasing in the interface inductance L_1 in Fig.1 can increase the associated capacitor of TLI to increase the errors, as shown in Fig.13, but it doesn't affect the errors of ITI. Besides, The errors of MTI increase, reaching around 0.015%.

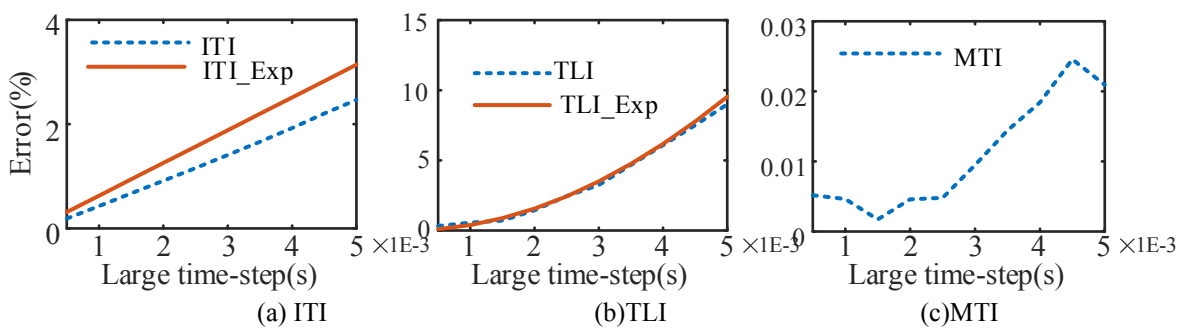

Fig. 10 Error evaluation using various large time-steps.

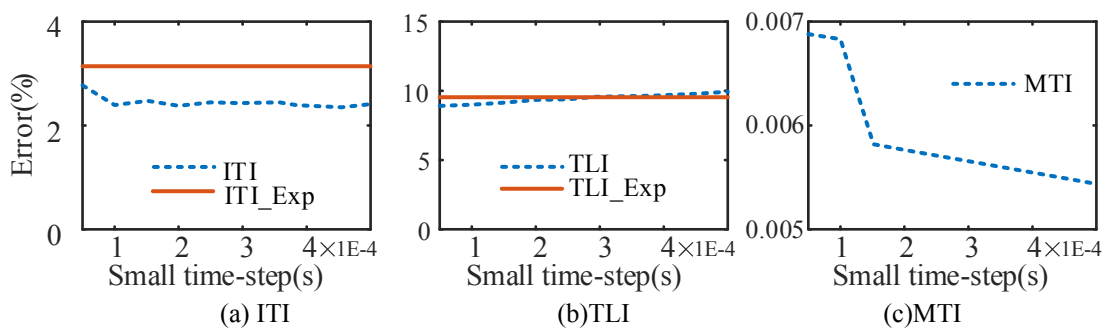

Fig. 11 Error evaluation using various small time-steps.

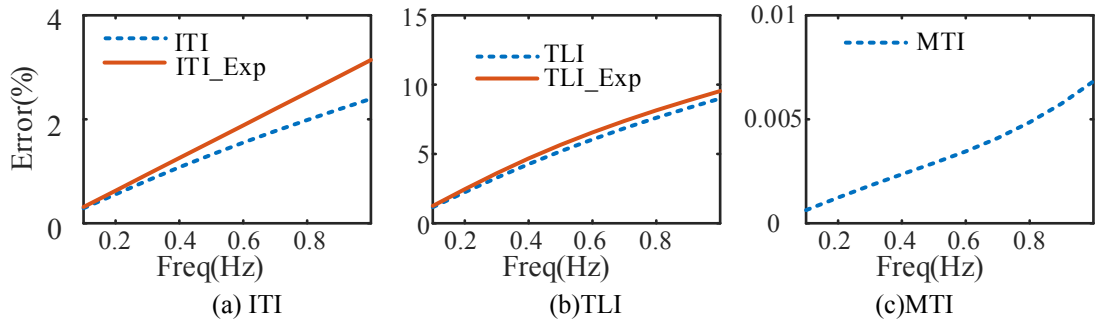

Fig. 12 Error evaluation using various frequencies.

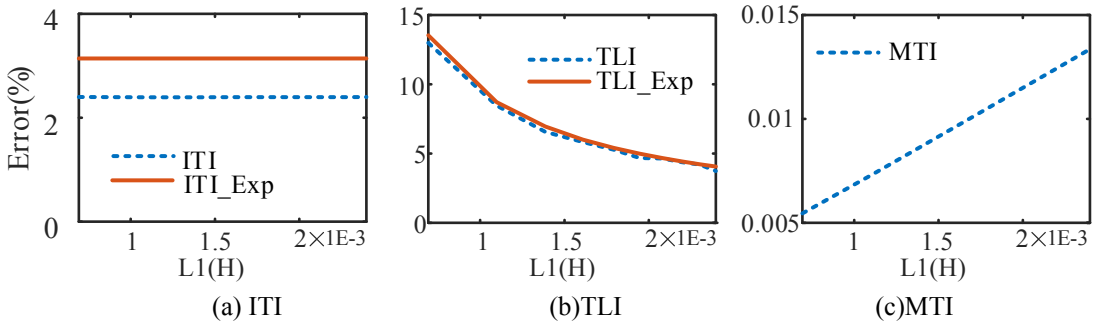

Fig. 13 Error evaluation using various connected inductors.

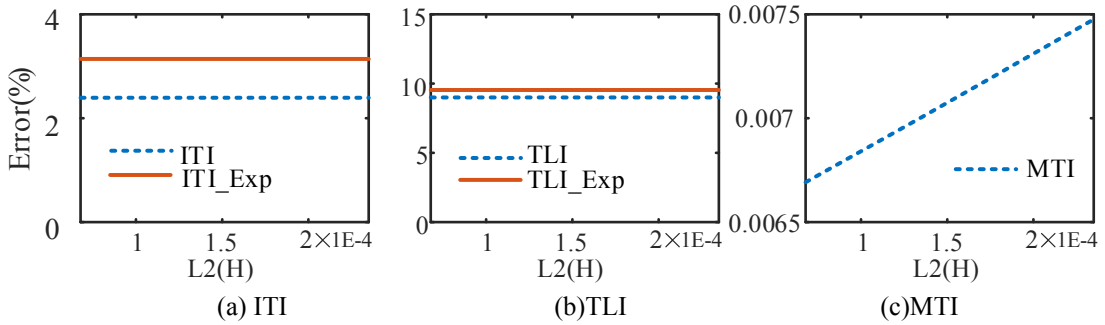

Fig. 14 Error evaluation using various inductors in the network with a large time-step.

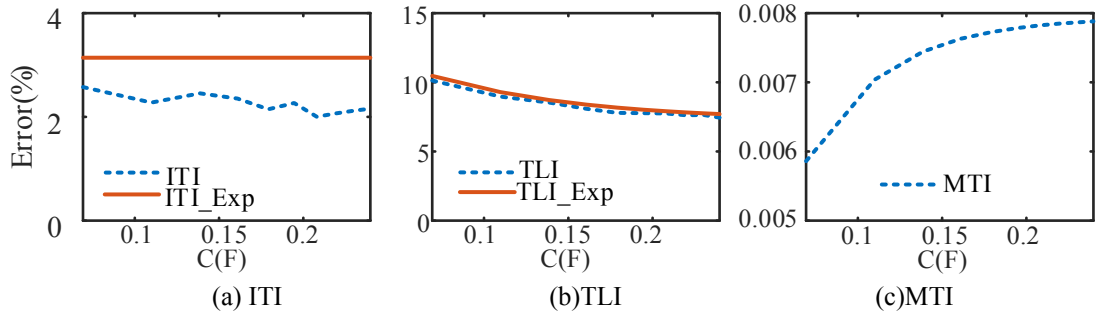

Fig. 15 Error evaluation using various capacitors in the network with a small time-step.

Increasing of the inductor L_2 in Fig.1 can increase the time constant in the large time-step subsystem, while the capacitor C_1 can increase the time constant in the small time-step subsystem. The results, as shown in Fig.14 and Fig.15, show the expected errors of ITI and TLI are close to the simulation errors, which means the errors of evaluation are sensible.

4.3. Unstable Case Study

The accuracy consists of two parts: error range induced by modelling simplification at each step and error accumulation throughout simulation which is defined as the stability of a simulation algorithm. Errors using the MTI are much smaller than using the ITI and TLI, because the MTI does not need simplification. In addition, the MTI is more stable than the ITI and TLI, so that the rate of error accumulation of MTI is slower than the other two methods for an unstable case. Therefore, the simulation accuracy of the MTI is always higher than the ITI and TLI.

Although the stability of the MTI has not been proved for unstable systems, simulation using the MTI for unstable systems is acceptable, because the MTI achieves smaller errors than the ITI and TLI which have already been widely used for practical applications.

In order to study the performance of the MTI for unstable systems, the example system has been modified to become unstable. The detailed parameters are listed in Appendix C.

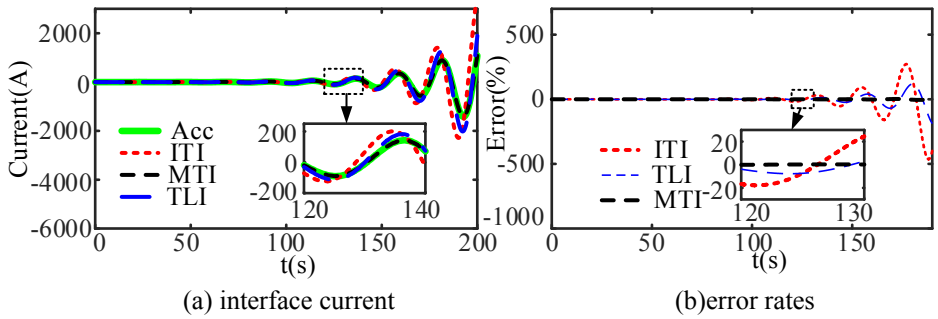

(a) interface current (b)error rates

Fig. 16 Error evaluation of an unstable system. (a) interface current; (b)error rates

In Fig.16, the original system is unstable, and the interface current, i_f, is increasing with oscillation. The MTI curve and the accurate result (Acc) are in agreement in Fig.16(a). The ITI and TLI can generate larger errors. The error rate (the difference between the accurate results and multi-rate results divided by RMS of the accurate results) is illustrated in Fig.16(b). The error rates of the ITI and TLI increases as the simulation proceeds, while the error of the MTI almost doesn't increase. The results with the MTI follow the accurate results well, although the system itself is unstable.

5. Case Study

Although a linear system was used in theoretical analyses of multi-rate algorithms, the proposed multi-rate algorithm can be used for practical nonlinear systems with acceptable small errors, which are verified in this section.

This paper makes use of the multi-rate simulations to study the Zhou Shan Multi-terminal HVDC (MTDC) [33], as show in Fig.17.

The local AC power system, as shown in, includes 28 buses and 1 generators, the topology of DC system consists of 5 AC/DC converter stations connect AC system to DC system. Modular Multi-level Converters (MMC) are replaced by two-level converters, in order to avoid the influence of the complex modelling of MMC upon the evaluation.

It is noticed that only the TLI and MTI are studied, except ITI, which has experienced instability, as discussed in section III.

5.1. Simulation Speeds

The multi-rate simulation was carried out in Advanced Digital Power System Simulator (ADPSS). The original test system is divided into 6 subsystems. 5 DC subsystems with the boundary of grey dash lines are simulated with a small time-step, 2μs. One AC subnetwork with the boundary of deep dash lines is simulated with a large time-step, 50μs, as shown in Fig.16.

The detailed comparison of different dividing schemes is illustrated in Fig. 18. The label in the axis of X represents the division type, (number of AC subsystems + number of DC subsystems). The PSCAD software runs about 1860s for 1s period of simulation as the computation time base. When the system is divided into a fast system (DC) and a slow system (AC), the computation time for 1s period of simulation decreases to 273s using the TLI or 294s using the MTI. Thus, the rate of speed-up reaches 6.33 (1860/294) for MTI. When the system is divided into more subsystems with small time-steps, a higher rate of speed-up is obtained, which can be up to 64. However, if there are more than 6 subsystems, the speed of simulation improves insignificantly through increasing subsystems with small time-steps. Therefore, the dividing scheme is optimized, which has 5 DC subsystems and 1 AC subsystem.

When using multi-rate algorithms for real-time simulation, the costs of hardware, e.g. racks, processors or FPGAs, can be greatly

reduced for simulating large systems with more power electronics converters and with smaller time steps [34].

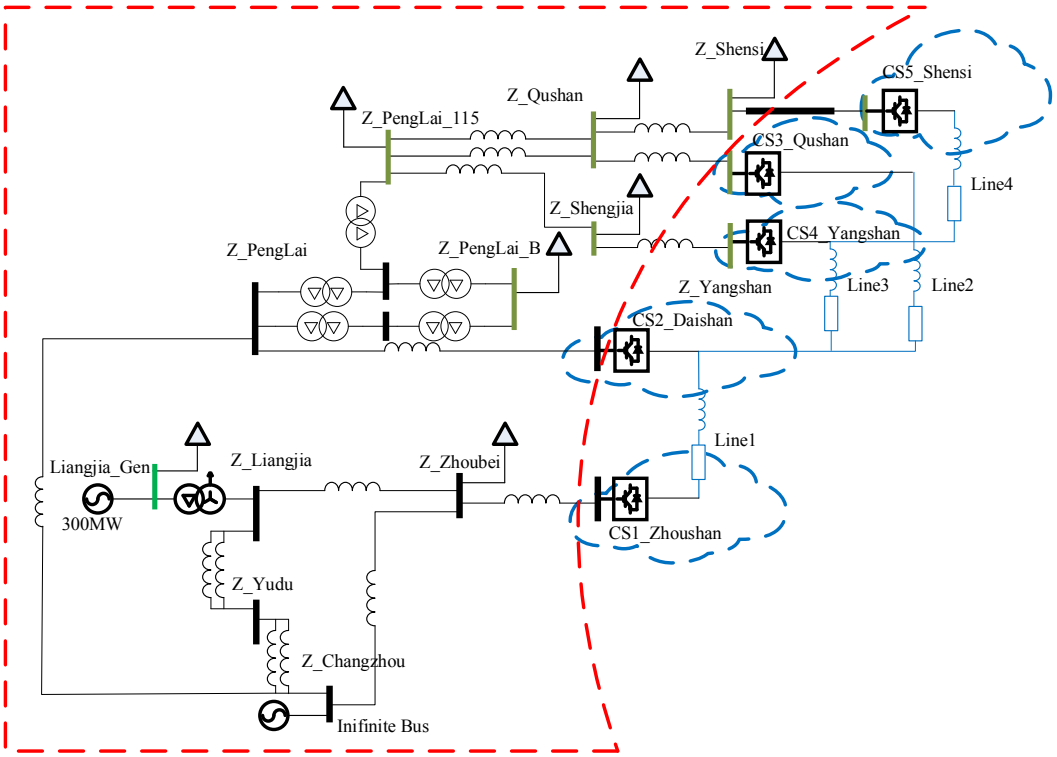

Fig. 17 System Topology of Zhou Shan MTDC.

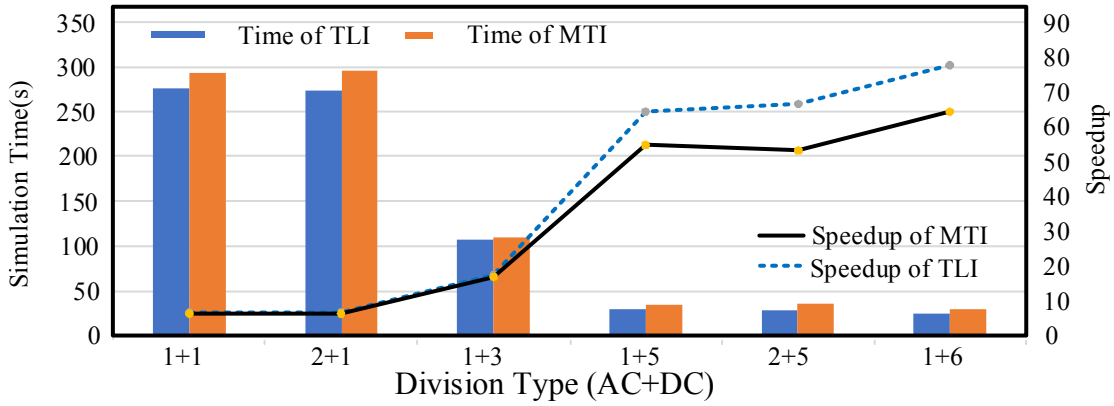

Fig. 18 Computation Time Comparison of different subsystem divivision types.

5.2. Accuracy Evaluation

The accuracy evaluation is to compare simulation results between non-partitioned system with a single time-step of 2μs and the partitioned system with different rates of 2μs and 50μs, as shown in Fig.19-20.

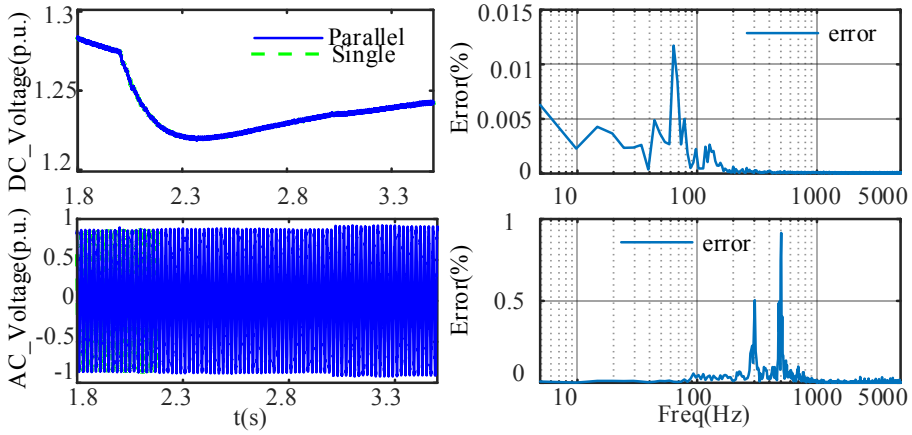

Fig. 19 Responses of the system with TLI.

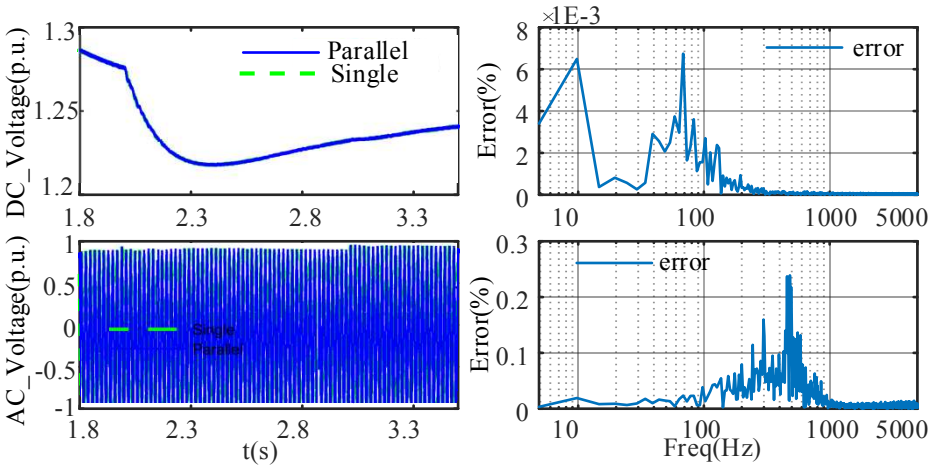

Fig. 20 Responses of the system with MTI.

In Fig 19 to 20, the first row represents the DC voltage of CS1, and the second row is the AC voltage of CS2. The errors expressed as a percentage are analyzed in frequency domain. It shows that all of errors are less than 1%. And the errors in the fundamental frequency are less than 0.03%. Comparing errors of the TLI and the MTI, the MTI has smaller than half of the errors of the TLI, thus the MTI is more accurate than the TLI.

6. Conclusion

With wide applications of IGBT-based power electronic devices in modern power systems, multi-rate simulation, as an expecting simulation technology, shows necessity for the simulation of large-scale power systems. This paper addresses the difficulties of using the multi-rate simulation.

The key findings of the study include

1. An improved method, Modified Thevenin Interface (MTI) is proposed to overcome the drawbacks in synchronization of the original Thevenin Interface.

2. Three theorems about ITI, TLI and MTI are proposed and proved in theoretically. From these theorems, it has been found that the stability of multi-rate simulation using these interfaces is only associated with the stability of single rate parallel simulation using these interfaces. The stability of MTI is only associated with the stability of the simulated case. Therefore, MTI performs higher stability and less limitation.

3. In terms of error analysis, the errors of ITI only depend on the delay introduced by the parallel algorithm, which are smaller than the errors of TLI.

4. The errors of TLI are dependent on the associated capacitor of TLI and the equivalent admittance of the subsystem from the

interface.

5. The errors of the MTI are convergent and much smaller than the previous two.

Through the proposed theorems and methods, the accuracy and stability of the multi-rate parallel simulation of DC grids are able to be evaluated conveniently. Multi-rate simulation has been performed to analyze the practical project, Zhoushan MTDC in China, which presents high speed and accuracy. The suitable multi-rate simulation algorithm can be applied in the analysis of DC grids to achieve fast and accurate simulation results.

7. References

[1] ElectricityNetworksStrategyGroup. "Our electricity transmission network: a vision for 2020," March 2012, 2012; http://webarchive.nationalarchives.gov.uk/20100919181607/http:/www.ensg.gov.uk/assets/1696-01-ensg_vision2020.pdf.

[2] C. Von Hirschhausen, "Developing a "Super Grid": Conceptual Issues, Selected Examples, and a Case Study for the EEA-MENA Region by 2050 ("Desertec")," April, 2010, 2010.

[3] L. Snider, J. langer, and G. Nanjundaiah, "Today's power system simulation challenge: High-performance, scalable, upgradable and affordable COTS-based real-time digital simulators," in Proc. 2010 Joint International Conference on Power Electronics, Drives and Energy Systems (PEDES) & 2010 Power India 2010, pp. 1-10.

[4] U. D. Annakkage, N. K. C. Nair, Y. Liang, A. M. Gole, V. Dinavahi, B. Gustavsen, T. Noda, Hassan Ghasemi, A. Monti, M. Matar, R. Iravani, and J. A. Martinez, "Dynamic System Equivalents: A Survey of Available Techniques," *IEEE Trans. Power Del.,* vol. 27, no. 1, pp. 411-420, Jan, 2012.

[5] H. Dommel, *Electromagnetic Transients Program Reference Manual*, Portland, OR: Bonneville Power Administration, 1986.

[6] A. M. Gole, "Electromagnetic transient simulation of power electronic equipment in power systems: challenges and solutions," in Proc. 2006 IEEE Power Engineering Society General Meeting, 2006, pp. 6 pp.

[7] D. M. Falcao, E. Kaszkurewicz, and H. L. S. Almeida, "Application of parallel processing techniques to the simulation of power system electromagnetic transients," *IEEE Trans. Power Syst.,* vol. 8, no. 1, pp. 90-96, Feb, 1993.

[8] W. Gropp, "MPI 3 and Beyond: Why MPI Is Successful and What Challenges It Face," in Proc. 19th European MPI Users' Group Meeting, EuroMPI 2012, 2012, pp.

[9] J. G. Pearce, R. E. Crosbie, J. J. Zenor, R. Bednar, D. Word, and N. G. Hingorani, "Developments and Applications of Multi-rate Simulation," in Proc. 11th International Conference on Computer Modelling and Simulation UKSIM '09, 2009, pp. 129-133.

[10] L. Li, W. N. Fu, S. L. Ho, Niu Shuangxia, and Li Yan, "A Quantitative Comparison Study of Power-Electronic-Driven Flux-Modulated Machines Using Magnetic Field and Thermal Field Co-Simulation," *IEEE Trans. Ind. Electron.,* vol. 62, no. 10, pp. 6076-6084, 2015.

[11] X. Sun, and M. Cheng, "Thermal Analysis and Cooling System Design of Dual Mechanical Port Machine for Wind Power Application," *IEEE Trans. Ind. Electron.,* vol. 60, no. 5, pp. 1724-1733, May, 2013.

[12] M. Valenzuela Guzman, and M. A. Valenzuela, "Integrated Mechanical-Electrical Modeling of an AC Electric Mining Shovel and Evaluation of Power Requirements During a Truck Loading Cycle," *IEEE Trans. Ind. Appl.,* vol. 51, no. 3, pp. 2590-2599, May, 2015.

[13] X. Zhang, "Multiterminal voltage-sourced converter-based HVDC models for power flow analysis," *IEEE Trans. Power Syst.,* vol. 19, no. 4, pp. 1877-1884, Nov., 2004.

[14] J. Beerten, S. Cole, and R. Belmans, "A sequential AC/DC power flow algorithm for networks containing Multi-terminal VSC HVDC systems," in 2010 IEEE Power and Energy Society General Meeting, 2010, pp. 1-7.

[15] M. Amini, A. I. Sarwat, S. S. Iyengar, and I. Guvenc, "Determination of the minimum-variance unbiased estimator for DC power-flow estimation," in IECON 2014 - 40th Annual Conference of the IEEE Industrial Electronics Society, 2014, pp. 114-118.

[16] K. G. Boroojeni, M. Hadi Amini, and S. S. Iyengar, "Error Detection of DC Power Flow Using State Estimation," *Smart Grids: Security and Privacy Issues*, pp. 31-51, Cham: Springer International Publishing, 2017.

[17] M. H. Amini, M. Rahmani, K. G. Boroojeni, G. Atia, S. S. Iyengar, and O. Karabasoglu, "Sparsity-based error detection in DC power flow state estimation," in 2016 IEEE International Conference on Electro Information Technology (EIT), 2016, pp. 0263-0268.

[18] M. H. Amini, R. Jaddivada, S. Mishra, and O. Karabasoglu, "Distributed security constrained economic dispatch," in 2015 IEEE Innovative Smart Grid Technologies - Asia (ISGT ASIA), 2015, pp. 1-6.

[19] S. Lefebvre, W. K. Wong, J. Reeve, M. Baker, and D. Chapman, "Considerations for modeling MTDC systems in transient stability programs," *IEEE Trans. Power Del.,* vol. 6, no. 1, pp. 397-404, 1991.

[20] P. Mahdavipour Vahdati, A. Kazemi, M. H. Amini, and L. Vanfretti, "Hopf Bifurcation Control of Power Systems Nonlinear Dynamics Via a Dynamic State Feedback Controller--Part I: Theory and Modelling," *IEEE Trans. Power Syst.,* vol. PP, no. 99, pp. 1-1, 2017.

[21] M. Saeedifard, M. Graovac, R. F. Dias, and R. Iravani, "DC power systems: Challenges and opportunities," in Power and Energy Society General Meeting, 2010 IEEE, 2010, pp. 1-7.

[22] J. Cronin, R.E. O'Malley, and American Mathematical Society, *Analyzing Multiscale Phenomena Using Singular Perturbation Methods: American Mathematical Society Short Course, January 5-6, 1998, Baltimore, Maryland*: American Mathematical Society, 1999.

[23] W. Ren, M. Steurer, and T. L. Baldwin, "Improve the Stability and the Accuracy of Power Hardware-in-the-Loop Simulation by Selecting Appropriate Interface Algorithms," *IEEE Trans. Ind. Appl.,* vol. 44, no. 4, pp. 1286-1294, July, 2008.

[24] S. Y. R. Hui, K. K. Fung, and C. Christopoulos, "Decoupled simulation of DC-linked power electronic systems using transmission-line links," *IEEE Trans. Power Electron.,* vol. 9, no. 1, pp. 85-91, Jan, 1994.

[25] F. Moreira, and J. Marti, "Latency techniques for time-domain power system transients simulation," in Proc. 2005 IEEE Power Engineering Society General Meeting, 2005, pp. 1383-1383.

[26] J. Chen, and M. L. Crow, "A Variable Partitioning Strategy for the Multirate Method in Power Systems," *IEEE Trans. Power Syst.,* vol. 23, no. 2, pp. 259-266, May, 2008.

[27] D. Word, John J. Zenor, R. Bednar, R. E. Crosbie, and N. G. Hingorani, "Multi-rate real-time simulation techniques," in Proc. 2007 Summer Computer Simulation Conf., 2007, pp. 195-198.

[28] R. Bednar, and R. E. Crosbie, "Stability of multi-rate simulation algorithms," in Proc. 2007 Summer Computer Simulation Conf., 2007, pp. 189-194.

[29] E. Isaacson, and H.B. Keller, *Analysis of Numerical Methods*, p.^pp. 401: Dover Publications, 2012.

[30] S. Skelboe, "Stability properties of backward differentiation multirate formulas," *Applied Numerical Mathematics,* vol. 5, no. 1–2, pp. 151-160, Feb, 1989.

[31] C.T. Chen, *Linear System Theory and Design*, Oxford: Oxford University Press, 2009.
[32] Q. Mu, "Study on Multi-rate Electromagnetic Transient Simulation Algorithm for the Power System with Multiple Voltage Source Converters," Ph.D, China Electric Power Research Institute, 2013.
[33] F. Wu, Y. Ma, N. Mei, and X. Zou, "Design of Main Connection Scheme for Zhoushan Flexible Multi-Terminal HVDC Transmission Project," *Power System Technology,* vol. 38, no. 10, pp. 2651-2657, Oct, 2014.
[34] L. Jiadai, and V. Dinavahi, "A Real-Time Nonlinear Hysteretic Power Transformer Transient Model on FPGA," *IEEE Trans. Ind. Electron.,* vol. 61, no. 7, pp. 3587-3597, 2014.

8. APPENDIX

8.1. Parameters of Zhoushan MTDC

Some parameters of VSC-MTDC in Fig. 17 on the large case study are listed as below, the detailed information refers to [33].

Transmission Lines: *Line 1=46km, Line 2=17km, Line 3=39km, Line 4=32.3km R=0.0192ohm/km, L=0.24mH/km, C =0.2961uF/km.*

Converters:

Zhoushan (CS1) (VQ mode), V=±200kV, Q=60MVar Capacitor=432uF; Leakage reactance= 14.098%; MVA rating = 450MVA

Daishan (CS2) (PQ mode), P=-200MW, Q=60MVar; Capacitor= 432uF; Leakage reactance= 14.98 %; MVA rating = 350MVA

Qushan (CS3) (PQ mode), P=80MW, Q=20MVar; Capacitor= 108uF; Leakage reactance= 14.8 %; MVA rating = 120MVA

Yangshan (CS4) (PQ mode), P=80MW, Q=20MVar; Capacitor= 144uF; Leakage reactance= 14.8 %; MVA rating = 120MVA

Shensi (CS5) (PQ mode), P=80MW, Q=20MVar; Capacitor= 144uF; Leakage reactance= 14.8 %; MVA rating = 120MVA

Topology of Converters:

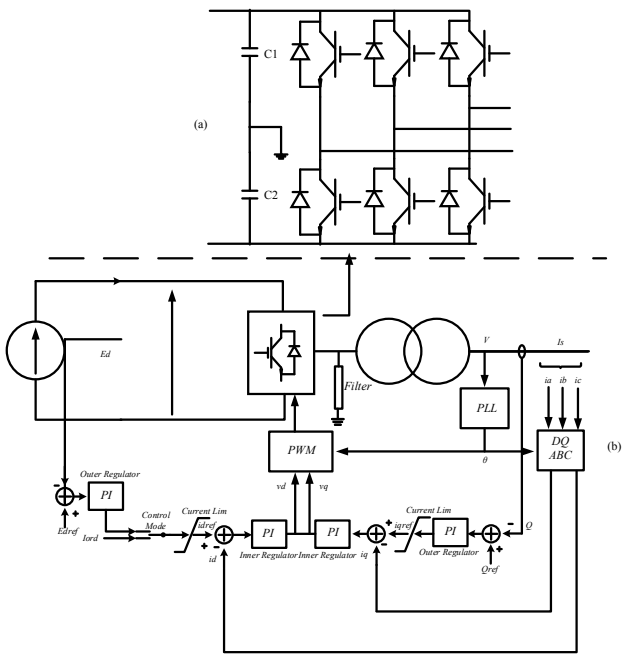

Controller parameters for CS1 to CS5:

Id/Iq inner Loop Ti= 0.1075 Kp= 0.6907; Ed Outer loop Ti=0.2 Kp=2; Vac Outloop Ti=0.4 Kp=2;

Filter: *R=10Ω L=3H*

8.2. Parameters of Power Systems in ZhouShan MTDC

Infinite Bus:

Vbase	Vac	Phase	R	L
230kV	0.991244p.u.	-26.415037	0.002p.u.	0.02p.u.

AC Transformer:

Station	MVA rating	Voltage	Leakage Reactance	Resistance
LiangJia	360MW	236/20	0.018610*2	0.000295*2
Penglai1	180MW	230/230	0.041950*2	0.000515*2

Penglai2	180MW	230/230	0.041950*2	0.000515*2
Penglai_B1	72MW	230/37	0.026650*2	0.000570*2
Penglai_B2	72MW	230/37	0.026650*2	0.000570*2
Penglai_115	180MW	226/115	0.003001*2	0.000290*2

Load Condition

Station	Rating Voltage (p.u.)	Active Power (p.u.)	Reactive Power (p.u.)	MVA Base	kV Base
ZhouBei	0.9715	0.6195	0.1405	100	230.00
LiangJia	1	0.21	0.1	100	20.0
Penglai_115	0.94335	0.3280	0.16400	100	37.0
Penglai_B	0.961	0.47710	0.15760	100	115
Shengjia	0.9804	0.2301	0.2454	100	115
Qushan	0.9638	0.20530	0.0492	100	115
Shensi	0.97125	0.2616	0.4013	100	115

Gen Model (LiangJia_GEN)

Power Rating	300MW	V RMS	20kV		
Stator resistance	0.001p.u.	Leakage inductance	0.174	Inertia constant	5.269s
Xd(p.u.)	1.86	Xd'(p.u.)	0.229	Xd''(p.u.)	0.174
Xq(p.u.)	1.75	Xq'(p.u.)	0.382	Xq''(p.u.)	0.174
Td0'	8.6s	Td0''	0.044s		
Tq0'	0.96s	Tq0''	0.074s		

Governing and Turbines(Type 1)

Valve Position Up limit	1	Valve Position Down limit	0.01	Opening Rate Limit	1.0
Closing Rate Limit	-1.0	Dead band	0.001	Speed Relay	0.1s
Coefficient of Speed governor	20	Time constant of main inlet volumes and steam chest	0.2s	Time constant of reheater	10s
Fraction of HP	0.333				

Excitation Systems (Type 1)

Amplifier	10	Time constant	0.01s	Maximum of field voltage	21.5p.u.
Minimum of field voltage	-21.5p.u.	Time constant of excitation	0.1s	Proportional coefficient of excitation	1.0
Coefficient of Speed governor	20	Compensation Coefficient	0.001		

Line Parameters (MVA Base = 100MVA)

Where CZ is the abbreviation of Z_Changzhou, YD is abbreviation of Z_Yidu, PL is the abbreviation of Z_Penglai, ZB is the abbreviation of Zhoubei, LJ is the abbreviation of Z_Liangjia, CS represents the converter station, SJ is the abbreviation of Shengjia, QS is the abbreviation of Z_Qushan, SS is the abbreviation of Z_Shensi.

	R+ (p.u.)	L+ (p.u.)	C+ (p.u.)	R0 (p.u.)	L0 (p.u.)	C0 (p.u.)	RMS (kV)
CZ-YD 1	0.0017	0.0129	0.0299	0.0129	0.0375	0.0204	230
CZ-YD 2	0.0017	0.0129	0.0299	0.0129	0.0375	0.0204	230
CZ-PL	0.0058	0.0276	0.0327	0.0385	0.0713	0.0222	230
CZ-ZB	0.0015	0.0111	0.0190	0.0110	0.0324	0.0129	230
YD-LJ1	0.0013	0.0097	0.0167	0.0096	0.0284	0.0113	230
YD-LJ2	0.0013	0.0097	0.0167	0.0096	0.0284	0.0113	230
ZB-LJ	0.0019	0.0145	0.0248	0.0143	0.0423	0.0169	230
ZB-CS1	0.0075	0.0295	0.0000	0.0458	0.0706	0.0000	230
PL-CS2	0.0075	0.0295	0.0000	0.0458	0.0706	0.0000	230
PL_115-SJ	0.0399	0.0691	0.1195	0.1367	0.0926	0.0813	115
PL_115-QS1	0.0081	0.0303	0.0432	0.0483	0.0707	0.0294	115
PL115-QS2	0.0081	0.0303	0.0432	0.0483	0.0707	0.0294	115
SJ-CS4	0.0035	0.0145	0.0000	0.0219	0.0355	0.0000	115
QS-SS	0.0360	0.0591	0.1195	0.1177	0.0756	0.0813	115
QS-CS3	0.0075	0.0295	0.0000	0.0458	0.0706	0.0000	115
SS-CS5	0.0025	0.0095	0.0000	0.0150	0.0223	0.0000	115

8.3. Parameters of the unstable case study

Parameters of the circuit

R_1	5000Ω	R_2	1Ω
R_3	4Ω	R_4	-0.76Ω
R_{brk}	0.1Ω		
C	30F	L_1	0.3H
L_2	0.03H	L_{TLI}	0.2H
V_s	sin(1*2πt)V		

Highlights

- Three theorems for the stability of three typical multi-rate simulation algorithms have been proposed and proved.
- The error of three typical multi-rate simulation algorithms has been modelled.
- The backward synchronization for the Thevenin equivalent interface has been proposed to overcome the challenge of synchronization.
- Three typical multi-rate simulation algorithms have been compared to illustrate that the modified Thevenin equivalent interface is the most stable and accurate.
- The multi-rate simulation algorithm has been used in the studies of DC grids, which achieve the great improvement of the simulation speed.